

Apportionment of PM_{2.5} Sources across Sites and Time Periods: An Application and Update for Detroit, Michigan

Zhiyi Yang ¹, Md Kamrul Islam ², Tian Xia ² and Stuart Batterman ^{2,*}

Supplemental Information

February 2023

Contents

S1. PMF background and model construction	2
S2. Pandemic related changes in pollutant levels, trends and apportionments.....	3
S3. Supplemental figures and tables	5

List of Tables

Table S1. Summary statistics for reconstructed and measured PM _{2.5} concentrations.....	5
Table S2. Summary statistics of PM _{2.5} and other species at the three monitoring sites ($\mu\text{g}/\text{m}^3$).....	7
Table S3. Comparisons between pairs of sites for concentrations of PM _{2.5} and other species.	9
Table S4. Concentrations at the three sites for one-year periods before and during the pandemic.	10
Table S5. Selected profiles from EPA Speciate database. In percent. Continued on next page.....	31
Table S6. Facility emissions of PM _{2.5} and PM ₁₀ for 50 largest point sources in Wayne County.	33
Table S7. Facility emissions of NO _x and SO ₂ for top 50 sources in Wayne County.	34
Table S8. Facility emissions of CO and VOCs of top 50 sources in Wayne County.	35

List of Figures

Figure S1. Scatterplots of reconstructed versus measured PM _{2.5} concentrations.....	6
Figure S2. Trends of monthly median levels of selected species for 1-year pre-pandemic and pandemic periods at Allen Park.....	13
Figure S3. Trends of monthly median concentrations selected species for 1-year pre-pandemic and pandemic periods at Dearborn.	14
Figure S4. Trends of monthly median concentrations for selected species for 1-year pre-pandemic and pandemic periods at SWHS.	15
Figure S5. Density plots comparing before and during the pandemic periods for selected species at Allen Park. ..	16
Figure S6. Density plots comparing before and during the pandemic periods for selected species at Dearborn.	19
Figure S7. Density plots comparing before and during the pandemic periods for selected species at SWHS.	22
Figure S8. Factor profiles for approach 1 for pre-pandemic and lockdown periods at Allen Park.....	25
Figure S9. Factor profiles for approach 1 for pre-pandemic and pandemic periods at Dearborn.....	26
Figure S10. Factor profiles for approach 1 for pre-pandemic and pandemic periods at SWHS site.	27
Figure S11. Factor profiles of approach 2A and 3 for pre-pandemic and pandemic periods.....	28
Figure S12. Annual wind rose for Detroit City Airport (Jan. 1, 2017 to Dec. 31, 2021).	29
Figure S13. Seasonal wind roses for Detroit City Airport.	30
Figure S14. Michigan state-wide stationary (point) source emission trends from 1974 to 2018.....	36

S1. PMF background and model construction

1.1 General background

The following provides general background on PMF and receptor models. In brief, these techniques use the compositions of sources to identify and quantify the contribution of sources [1]. The chemical mass balance (CMB) model provides a solution to the apportionment problem if the source profiles are known [1,2]. This model has four assumptions: 1) compositions of sources do not change during the ambient and source sampling; 2) there is no reaction between chemical species; 3) sources of significant contributions for the receptor and their emission characteristics have been identified; 4) source profiles are linearly independent [2,3]. In the CMB model, mass concentrations of each species are considered as linear combination of emission source contributions [4]:

$$x_{ij} = \sum_{k=1}^p g_{ik} f_{kj} + e_{ij}$$

where, x_{ij} is the $i \times j$ dimensional data matrix of i samples and j species with uncertainties u ; p denotes the number of factors; f is the number of species profile of each source; g represents the contribution of each factor to an individual sample; and e is the residual for the sample.

Another approach to solve the equation above but in the case where the source profile matrix f is unknown, uses positive matrix factorization. Again, the sample data is divided into two matrices [5]: factor contribution and factor profile. Both matrices are solved by minimizing objective function Q below:

$$Q = \sum_{i=1}^n \sum_{j=1}^m \left[\frac{x_{ij} - \sum_{k=1}^p g_{ik} f_{kj}}{u_{ij}} \right]^2$$

where n denotes the number of samples, m is the number of species, p is the number of sources, and x_{ij} and u_{ij} refer to the concentration and the uncertainty of each sample. Q in the formula is a critical parameter. There are two versions of Q in the PMF model provided by US EPA [6]: $Q(\text{True})$ and $Q(\text{robust})$, which differ by the approach used to calculate goodness of fit parameters, e.g., including all points or excluding points not fit by the model.

Other approaches and extensions to RM provide apportionments that can assist in locating potential source areas. The use of RM with Potential Source Contribution Function (PSCF) can indicate a potential source region contributing to a high air pollutant concentration by using trajectories of air masses over a given geographic region that contain high air pollutant concentrations as measured at a receptor [7]. The use of Concentration Weighted Trajectory (CWT) models identifies potential source areas, also using trajectory analyses to weight grid cell by the air mass residence time [8].

1.2 Model construction and application

Parameter selection and procedures for the PMF models followed recent literature. Using the signal to noise ratio (S/N), each species was characterized as ‘bad’, ‘weak’ or ‘strong’ for $S/N < 0.5$, $0.5 \leq S/N < 1$, and $S/N \geq 1$, respectively [9]. For ‘weak’ species, uncertainties were increased 3-fold, and ‘bad’ species were excluded from further analysis, namely, Sb, Ba, Cd, Ce, Cs, In, Ru, Ag and Sn at all sites, additionally Co and V at DB and V at SWHS. Overall, the models used 26 species ($\text{PM}_{2.5}$, EC, OC, NH_4^+ , NO_3^- , SO_4^{2-} , S, Al, Br, Ca, Cl^- , Cr, Cu, Fe, K^+ , Mg, Mn, Na^+ , Ni, Pb, Se, Si, Sr, Ti, Zi, and Zn). To obtain a complete dataset, missing data were replaced using the median, negative values were set to 0, and uncertainties of missing and negative values were set to four times the median concentration [10,11,12]. Values below the MDL were replaced by $\frac{1}{2}$ MDL and assigned uncertainties of $5/6$ MDL [9,11,12,13]. The uncertainty of values exceeding the MDL was calculated using Gaussian quadrature to propagate fixed and proportional errors, the latter assuming a fractional error of 0.1 [6,11].

Several steps were used to clean and impute data. We checked for reasonable ranges and possible outliers of each

parameter by examining the highest values. Two observations with clear outliers were removed: 2/26/19 at SWHS with greatly elevated Al levels ($11.2 \mu\text{g}/\text{m}^3$) and somewhat elevated Si but otherwise typical levels; and 7/5/20 at AP with elevated levels of Al, Ba, Mg, K, S and other species; this date was considered by the State to reflect (distant) forest fires. (Measurements at the other sites were not collected on this date.) Na^+ measurements were missing for the initial 13 months of the study period; reconstructed $\text{PM}_{2.5}$ mass (RPM) depended on these missing measurements. To impute these measurements, available Na^+ data was regressed on Na ($\text{Na}^+ \approx 3.45 \text{ Na}$, $R^2=0.49$), and missing values were replaced with predictions. Next, FRM $\text{PM}_{2.5}$ measurements at each site were compared using scatterplots, ratios and other statistics to the RPM derived from elemental and ion measurements, which showed discrepancies for a number of observations (see the supplemental information for [Figure S1, Table S1](#)). Recognizing that relative error increases at low concentrations, several rules were used to identify and ultimately remove discordant observations: FRM < $1 \mu\text{g}/\text{m}^3$ with RPM > $4 \mu\text{g}/\text{m}^3$ or vice-versa (5 cases: 02/10/18, 09/12/20, 01/25/20 and 06/04/18 at AP; 09/10/17 at DB); FRM from $5\text{--}10 \mu\text{g}/\text{m}^3$ with relative deviation between FRM and RPM > 75% (4 cases: 12/17/19, 01/22/20, and 06/19/18 at AP; 06/17/16 at SWHS), and FRM > $10 \mu\text{g}/\text{m}^3$ with relative deviation above 50% (20 cases: 06/27/17, 12/01/18, 02/23/19, 10/17/18, 06/12/17, 01/18/19, 06/24/17, 06/30/19, 02/14/19, 09/02/19, 11/02/19 and 07/29/19 at AP; 08/11/17, 11/17/19 and 09/20/19 at SWHS; and 06/11/16, 03/07/16, 10/22/17, and 05/26/18 at DB). The PMF analyses used Na^+ , K^+ , and Cl^- instead of Na, K and Cl since they have a higher level of precision in analysis [15]. Species with detection frequencies below 25% of the method detection limit (MDL; [16]) were removed: As and P at all sites; Co and V at AP; and Co at SWHS. The number of daily observations in the final dataset was 693, 353 and 347 at AP, DB and SWHS, respectively.

S2. Pandemic related changes in pollutant levels, trends and apportionments.

This section extends the discussion of pandemic related effects. The discussion of the PMF profiles is limited to changes in profiles for approach 1. Approach 2A and 3 pool data across the time periods and therefore do not have experience shifts in the profiles (except between sites in approach 3). Approach 1 results are based on a smaller sample sizes, and the PMF models apply to a single year at each site. These factors limit comparability, although it is interesting to see the evolution of the profile.

At AP, decreases in annual average and median $\text{PM}_{2.5}$ levels during the pandemic appeared large ($\sim 1.5 \mu\text{g}/\text{m}^3$), but were not statistically significant. In addition to the decrease in EC levels, statistically significant decreases occurred for Ca, Fe and Mg, possibly reflecting less entrained soil due to diminished traffic and construction. Cu also decreased significantly, although levels were low and the monthly pattern was inconsistent. PMF profiles across the two periods were similar for non-ferrous metals, road salt, secondary nitrate and secondary sulfate profiles, but difference for ferrous metals (more Cr and Ni during the pandemic), mobile sources (more Al; less Pb, Zn), and secondary sulfate (more NH_4^+ , S; less Cr, Ni, K^+). While the dominant markers for each source type, the general pattern for other species, and the three top contributors (mobile, secondary sulfate and secondary nitrate) were unchanged across pre- and pandemic periods, the PMF models show large decreases ($>0.5 \mu\text{g}/\text{m}^3$) from mobile sources and ferrous metals, and increases from salt increased.

At DB, annual average $\text{PM}_{2.5}$ levels increased during the pandemic, but medians decreased; these changes were not statistically significant. In addition to lower EC levels, statistically significant decreases occurred at DB for Sb, Ca, Cu, Mn, Ru, Sn, Ti and Zn. The monthly plots suggest that Cu, Fe, Mn, Si and Zn fell in the ~ 6 months of the pandemic, possibly reflecting a slowdown in ferrous and non-ferrous metals production and processing. The density plots suggest shifts in distributions to lower values during the pandemic for EC, NH_4^+ , Sb, Pb, Sn, Ti and Zn; they also suggest (by extended right hand tails) higher peak values of $\text{PM}_{2.5}$, SO_4^{2-} , S, Na^+ and Cl^- during the pandemic. The PMF profiles showed changes for most sources, e.g., mobile sources (less Mg, S, SO_4^{2-} ; more Zn, Cr, EC in the pandemic period), secondary sulfate (more Mg, Ti, Zn, K^+ , NH_4^+ , S, SO_4^{2-} ; less Zn, Cr), secondary nitrate (more Zn, K^+), ferrous metals (more Fe, Ni; less Mn, Zn, Na^+ , K^+), soil/dust (more Sr, Al, Na^+), non-ferrous metals (more Cr; less Ni, Pb, Sr), and salt (more Na^+). These changes increased the apportionment of secondary nitrate and soil/dust; changes in other source contributions were small.

At SWHS, mean and median $\text{PM}_{2.5}$ levels appeared to fall during the pandemic, but again, these changes were not

significant. In addition to EC and OC, mean and/or median levels of NO_3^- , Fe, Cl⁻, Mn, K⁺ and Zn dropped during the pandemic, while levels of Ca, Cu, Si and Sr increased. The density plots suggest pandemic-related decreases in Pb and increases in Sb. The divergence in trends at SWHW suggests the influence of multiple source types, specifically, lower contributions of soil/dust (typically containing Ca, Si, Fe) during the pandemic, and higher contributions from ferrous metals sources (Fe). This was reflected in the PMF results which showed differences in the profiles including secondary sulfate (more Zi, Br, Na⁺, NH₄⁺, S, SO₄²⁻), secondary nitrate (less NH₄⁺), mobile (more Si, Cr, Zi, Na⁺), non-ferrous metals (less Cu, Cr; more Pb), soil/dust (more Al, Ca, Mg, Mn, Se, Ti), ferrous metals (more Fe; less Al, Ti). Despite these many changes, the only large changes in the apportionments were decreases in ferrous metals and increases in nonferrous metals.

Overall, the lower EC levels at the three sites suggested reduced traffic; the change at the SWHS site also may reflect diminished construction activity (e.g., non-road diesel sources). However, the PMF models did not show meaningful drops in mobile source levels at DB and AP. Across the three sites, sulfate and nitrate had mostly small differences, probably because these secondary pollutants arise mostly from regional sources (e.g., coal-fired power plants) that were largely unchanged during the pandemic lock-down period. Several sources with smaller contributions in the PMF models showed larger changes, as noted above and in the text,. Changes could reflect actual pandemic-induced changes, or just typical annual fluctuations due to variability in meteorology and emissions. Overall in southwest Detroit, changes in pollutant levels were small and few were statistically significant and consistent across sites.

S3. Supplemental figures and tables

Table S1. Summary statistics for reconstructed and measured PM_{2.5} concentrations.

PM_{2.5} measured using federal reference method 88101, and method 88502 at the three monitoring sites ($\mu\text{g}/\text{m}^3$); Allen Park from Jan 1, 2016, to May 31, 2021, Dearborn, and Southwestern High School from Jan 1, 2016, to May 28, 2021, based on 24-hour average concentrations.

Sites	Variables	N	Mean	SD	Min	25th	50th	75th	Max
Allen Park	Reconstructed	395	7.25	4.1	1.75	4.45	6.16	8.89	27.04
	88101	1303	8.74	4.65	0.2	5.5	7.8	10.9	41.9
	88502	1125	8.81	3.45	2	6	8	10	39
Dearborn	Reconstructed	200	8.83	4.82	2.04	5.52	7.84	11.05	29.9
	88101	1053	9.65	5.04	1.2	6.2	8.8	11.9	38.3
	88502	1292	9.71	3.89	3	7	9	12	39
Southwestern High School	Reconstructed	196	9.86	5.48	2.1	6.05	8.96	12.6	44.63
	88101	575	10.37	5.56	1.3	6.4	9.2	13.3	45.2

Figure S1. Scatterplots of reconstructed versus measured PM_{2.5} concentrations.
FRM measurements use methods 88101 and 88502, as available.

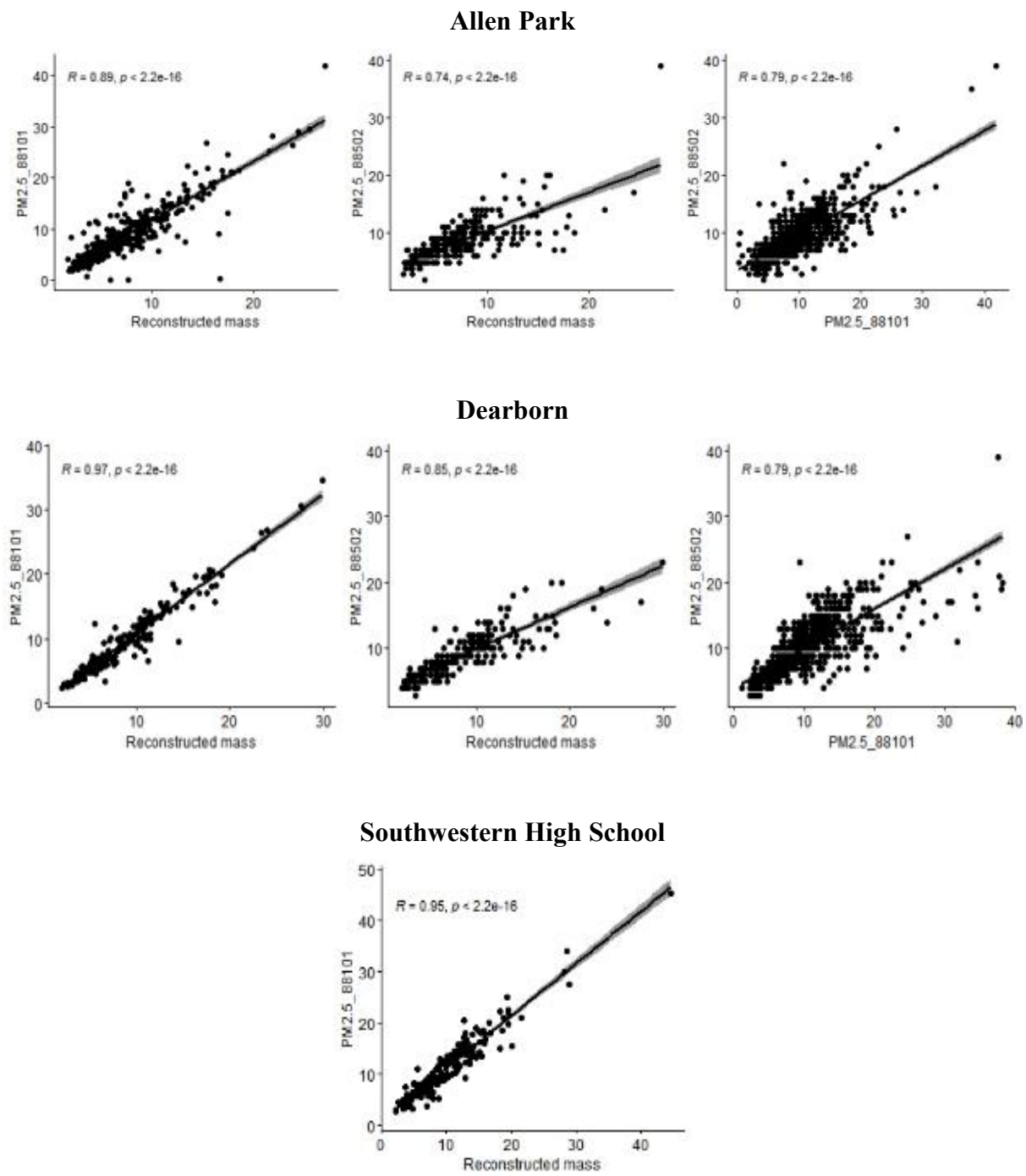


Table S2. Summary statistics of PM_{2.5} and other species at the three monitoring sites ($\mu\text{g}/\text{m}^3$).

Allen Park, Dearborn, and Southwestern High School from Jan. 1, 2016, to Dec. 31, 2021. Based on 24-hour average concentrations. Excludes for species with detection frequencies below 25% (of the MDL). Continued on 2 pages.

Site	Variable	Mean	SD	Min	25th	Median	75th	Max
Allen Park (N=693)	Al	0.02	0.04	-0.05	0.00	0.02	0.04	0.45
	NH ₄ ⁺	0.51	0.61	0.00	0.12	0.30	0.66	4.17
	Sb	0.00	0.01	-0.03	-0.01	0.00	0.01	0.06
	Ba	0.01	0.03	-0.07	-0.01	0.01	0.02	0.12
	Br	0.00	0.00	0.00	0.00	0.00	0.00	0.03
	Cd	0.00	0.01	-0.01	0.00	0.00	0.01	0.03
	Ca	0.07	0.07	0.00	0.03	0.05	0.08	0.60
	Ce	0.00	0.03	-0.07	-0.02	0.00	0.02	0.13
	Cl ⁻	0.08	0.19	-0.02	0.02	0.04	0.09	4.13
	Cs	0.00	0.02	-0.05	-0.01	0.00	0.02	0.09
	Cr	0.00	0.01	0.00	0.00	0.00	0.00	0.21
	Cu	0.01	0.01	-0.01	0.00	0.00	0.01	0.08
	EC	0.37	0.22	0.00	0.22	0.32	0.45	2.25
	In	0.00	0.01	-0.02	-0.01	0.00	0.01	0.05
	Fe	0.09	0.07	-0.02	0.05	0.07	0.11	0.78
	Pb	0.00	0.01	-0.01	0.00	0.00	0.01	0.03
	Mg	0.01	0.03	-0.02	0.00	0.01	0.03	0.21
	Mn	0.00	0.00	-0.01	0.00	0.00	0.00	0.01
	Ni	0.00	0.00	0.00	0.00	0.00	0.00	0.06
	OC	1.91	1.11	0.27	1.09	1.70	2.48	10.54
	K ⁺	0.04	0.07	0.00	0.01	0.02	0.04	1.39
	Ru	0.00	0.00	-0.01	0.00	0.00	0.00	0.01
	Se	0.00	0.00	0.00	0.00	0.00	0.00	0.01
	Si	0.06	0.07	-0.03	0.02	0.05	0.08	0.86
	Ag	0.00	0.01	-0.02	-0.01	0.00	0.01	0.03
	Na ⁺	0.04	0.11	-0.01	0.01	0.02	0.04	2.56
	Sr	0.00	0.00	0.00	0.00	0.00	0.00	0.05
	SO ₄ ²⁻	1.03	0.64	0.00	0.58	0.88	1.31	4.75
	S	0.38	0.24	0.00	0.21	0.33	0.49	1.67
	Sn	0.00	0.01	-0.03	-0.01	0.00	0.01	0.06
	Ti	0.00	0.00	0.00	0.00	0.00	0.01	0.03
	NO ₃ ⁻	1.50	1.89	-0.03	0.35	0.77	1.86	12.36
	Zn	0.02	0.01	0.00	0.01	0.01	0.02	0.15
	Zi	0.00	0.01	-0.03	-0.01	0.00	0.01	0.04
	PM _{2.5}	8.63	4.75	1.20	5.16	7.64	11.01	32.10
Dearborn (N=353)	Al	0.03	0.04	-0.04	0.00	0.02	0.05	0.28
	NH ₄ ⁺	0.58	0.61	0.00	0.16	0.40	0.75	4.02
	Sb	0.00	0.01	-0.03	-0.01	0.00	0.01	0.06
	Ba	0.01	0.03	-0.07	-0.01	0.00	0.03	0.12
	Br	0.00	0.00	0.00	0.00	0.00	0.00	0.04
	Cd	0.00	0.01	-0.02	0.00	0.00	0.01	0.03
	Ca	0.13	0.15	0.00	0.05	0.09	0.14	1.48
	Ce	0.01	0.03	-0.08	-0.01	0.01	0.03	0.12
	Cl ⁻	0.18	0.22	-0.01	0.04	0.11	0.23	2.56
	Cs	0.00	0.02	-0.05	-0.01	0.00	0.01	0.09
	Cr	0.00	0.01	0.00	0.00	0.00	0.00	0.12
	Co	0.00	0.00	0.00	0.00	0.00	0.00	0.01
	Cu	0.02	0.02	0.00	0.01	0.01	0.02	0.10
	EC	0.51	0.30	0.00	0.30	0.46	0.65	1.72
	In	0.00	0.01	-0.03	-0.01	0.00	0.01	0.03
	Fe	0.33	0.36	0.00	0.10	0.21	0.41	3.29
	Pb	0.01	0.01	-0.01	0.00	0.00	0.01	0.12

Mg	0.03	0.04	-0.02	0.00	0.02	0.04	0.27	
Mn	0.01	0.01	-0.01	0.00	0.01	0.01	0.05	
Ni	0.00	0.00	0.00	0.00	0.00	0.00	0.06	
OC	2.27	1.13	0.35	1.41	2.09	2.85	6.03	
K ⁺	0.05	0.06	0.00	0.02	0.03	0.06	0.74	
Ru	0.00	0.00	-0.01	0.00	0.00	0.00	0.01	
Se	0.00	0.00	0.00	0.00	0.00	0.00	0.01	
Si	0.08	0.09	-0.02	0.03	0.06	0.10	0.98	
Ag	0.00	0.01	-0.02	-0.01	0.00	0.01	0.02	
Na ⁺	0.05	0.06	0.00	0.02	0.03	0.07	0.31	
Sr	0.00	0.00	0.00	0.00	0.00	0.00	0.02	
SO ₄ ²⁻	1.24	0.71	0.01	0.66	1.10	1.70	3.63	
S	0.45	0.27	0.00	0.23	0.39	0.66	1.39	
Sn	0.00	0.01	-0.03	-0.01	0.00	0.01	0.06	
Ti	0.00	0.00	0.00	0.00	0.00	0.01	0.04	
NO ₃ ⁻	1.58	1.89	0.00	0.41	0.81	1.98	12.33	
V	0.00	0.00	0.00	0.00	0.00	0.00	0.02	
Zn	0.06	0.08	0.00	0.01	0.03	0.07	0.65	
Zi	0.00	0.01	-0.03	-0.01	0.00	0.01	0.04	
PM _{2.5}	9.88	5.37	1.15	5.85	9.25	13.00	34.65	
Al	0.07	0.20	-0.04	0.01	0.03	0.06	2.62	
NH ₄ ⁺	0.59	0.68	0.00	0.12	0.37	0.79	4.71	
Sb	0.00	0.01	-0.03	-0.01	0.00	0.01	0.05	
Ba	0.00	0.02	-0.06	-0.01	0.00	0.02	0.11	
Br	0.00	0.00	0.00	0.00	0.00	0.00	0.05	
Cd	0.00	0.01	-0.01	0.00	0.00	0.01	0.03	
Ca	0.16	0.22	0.00	0.05	0.09	0.18	1.87	
Ce	0.00	0.03	-0.06	-0.02	0.00	0.02	0.11	
Cl ⁻	0.20	0.26	-0.01	0.04	0.10	0.24	2.21	
Cs	0.00	0.02	-0.05	-0.01	0.00	0.01	0.09	
Cr	0.00	0.00	0.00	0.00	0.00	0.00	0.02	
Cu	0.01	0.01	0.00	0.01	0.01	0.01	0.07	
EC	0.61	0.41	0.04	0.33	0.50	0.77	3.21	
In	0.00	0.01	-0.03	-0.01	0.00	0.01	0.03	
Fe	0.17	0.16	0.01	0.08	0.11	0.21	0.89	
Pb	0.01	0.01	-0.01	0.00	0.00	0.01	0.04	
Southwestern High School (N=347)	Mg	0.03	0.06	-0.02	0.00	0.01	0.04	0.88
	Mn	0.01	0.01	0.00	0.00	0.00	0.01	0.03
	Ni	0.00	0.00	0.00	0.00	0.00	0.00	0.01
	OC	2.42	1.23	0.36	1.49	2.19	3.10	8.41
	K ⁺	0.08	0.18	0.00	0.02	0.03	0.07	2.49
	Ru	0.00	0.00	-0.01	0.00	0.00	0.00	0.01
	Se	0.00	0.00	0.00	0.00	0.00	0.00	0.01
	Si	0.11	0.13	-0.01	0.04	0.07	0.14	0.92
	Ag	0.00	0.01	-0.02	-0.01	0.00	0.01	0.03
	Na ⁺	0.04	0.06	-0.01	0.01	0.03	0.06	0.63
	Sr	0.00	0.00	0.00	0.00	0.00	0.00	0.02
	SO ₄ ²⁻	1.31	0.83	0.00	0.69	1.11	1.81	4.06
	S	0.46	0.29	0.00	0.23	0.41	0.64	1.45
	Sn	0.00	0.01	-0.03	-0.01	0.00	0.01	0.08
	Ti	0.01	0.02	-0.01	0.00	0.00	0.01	0.31
	NO ₃ ⁻	1.62	1.91	0.03	0.45	0.85	1.92	11.98
	V	0.00	0.00	0.00	0.00	0.00	0.00	0.01
	Zn	0.03	0.04	0.00	0.01	0.02	0.03	0.46
	Zi	0.00	0.01	-0.03	-0.01	0.00	0.01	0.05
	PM _{2.5}	10.83	5.48	1.30	6.55	10.00	13.95	33.86

SD: standard deviation; Min: minimum; 25th: 25th percentile; 75th: 75th percentile; Max: maximum.

Table S3. Comparisons between pairs of sites for concentrations of PM_{2.5} and other species.

Sites	Pollutants	Unpaired t-test		Mann-Whitney U test	
		T	p value	W	p value
Allen Park versus Dearborn	PM _{2.5}	-3.72	<0.01*	103499	<0.01*
	EC	-7.76	<0.01*	79609	<0.01*
	OC	-4.74	<0.01*	93280	<0.01*
	NH ₄ ⁺	-1.57	0.12	110283	0.02
	NO ₃ ⁻	-0.68	0.50	114861	0.20
	SO ₄ ²⁻	-4.72	<0.01*	99305	<0.01*
	S	-3.99	<0.01*	104496	<0.01*
Allen Park versus Southwestern High School	PM _{2.5}	-6.36	<0.01*	88194	<0.01*
	EC	-9.85	<0.01*	66265	<0.01*
	OC	-6.38	<0.01*	85211	<0.01*
	NH ₄ ⁺	-1.69	0.09	111415	0.09
	NO ₃ ⁻	-0.98	0.33	110136	0.05*
	SO ₄ ²⁻	-5.59	<0.01*	96016	<0.01*
	S	-4.44	<0.01*	101804	<0.01*
Dearborn versus Southwestern High School	PM _{2.5}	-2.28	0.02*	53329	0.01
	EC	-3.46	<0.01*	50731	<0.01*
	OC	-1.69	0.09	53746	0.10
	NH ₄ ⁺	-0.20	0.84	62224	0.67
	NO ₃ ⁻	-0.27	0.79	59400	0.53
	SO ₄ ²⁻	-1.21	0.23	59604	0.58
	S	-0.60	0.55	60653	0.82

*: P<=0.05, significant

Table S4. Concentrations at the three sites for one-year periods before and during the pandemic.
 Sample size: 116, 61 and 58 at AP, DB, SWHS before the pandemic, respectively, and 117, 60 and 58 during the pandemic. * denotes statistical significance with $P \leq 0.05$. Highlights show increases (pink) and decreases (blue).
 Continued on 3 pages.

Site	Pollutant	Mean ($\mu\text{g}/\text{m}^3$)		Median ($\mu\text{g}/\text{m}^3$)		Unpaired t-test		Mann-Whitney U test	
		Before	During	Before	During	t	p value	W	P-value
Allen Park	PM _{2.5}	8.275	8.105	6.850	6.710	0.26	0.80	6330.5	0.38
	EC	0.440	0.421	0.402	0.318	0.55	0.58	5668.5	0.04*
	OC	1.768	1.863	1.568	1.577	-0.68	0.50	6678	0.92
	NH ₄ ⁺	0.526	0.580	0.300	0.295	-0.61	0.54	6908	0.73
	NO ₃ ⁻	1.571	1.643	0.845	0.735	-0.27	0.79	6690	0.94
	SO ₄ ²⁻	0.887	1.012	0.730	0.885	-1.62	0.11	7486.5	0.14
	S	0.323	0.357	0.273	0.301	-1.22	0.22	7173	0.45
	Al	0.021	0.020	0.018	0.016	0.25	0.80	6825	0.94
	Sb	0.001	0.003	0.001	0.003	-1.37	0.17	7537.5	0.14
	Ba	0.005	0.006	0.004	0.006	-0.29	0.77	6899	0.83
	BC	0.481	0.308	0.421	0.213	4.23	<0.01*	3950	<0.01*
	Br	0.000	0.001	0.000	0.000	-0.30	0.77	7291	0.15
	Cd	0.002	0.002	0.001	0.001	0.21	0.83	6714.5	0.89
	Ca	0.090	0.057	0.055	0.041	3.16	<0.01*	5331.5	<0.01*
	Ce	0.001	0.000	-0.003	-0.002	0.56	0.57	6663	0.81
	Cl ⁻	0.102	0.090	0.048	0.047	0.73	0.47	6157.5	0.22
	Cs	0.002	0.002	-0.001	0.002	-0.02	0.98	6945	0.76
	Cr	0.002	0.002	0.001	0.001	1.02	0.31	6747.5	0.94
	Cu	0.007	0.004	0.004	0.002	2.59	0.01*	5487.5	0.01*
	In	0.001	0.003	0.000	0.003	-1.20	0.23	7643.5	0.10
	Fe	0.097	0.067	0.080	0.058	3.88	<0.01*	5077	<0.01*
	Pb	0.003	0.003	0.002	0.003	-0.98	0.33	7627	0.10
	Mg	0.021	0.011	0.017	0.000	3.20	<0.01*	4929	<0.01*
	Mn	0.003	0.002	0.002	0.002	2.05	0.04*	5945.5	0.10
	Ni	0.001	0.001	0.001	0.001	0.67	0.50	6681.5	0.83
	K ⁺	0.035	0.044	0.030	0.030	-1.14	0.26	7406	0.18
	Ru	0.000	0.000	0.000	0.000	-1.28	0.20	7440.5	0.20
	Se	0.001	0.001	0.000	0.001	0.09	0.93	6994.5	0.68
	Si	0.074	0.056	0.044	0.042	1.90	0.06	6364	0.41
	Ag	0.001	0.001	0.000	0.000	-0.27	0.79	6933	0.78
	Na ⁺	0.035	0.027	0.020	0.020	1.20	0.23	6361	0.46
	Sr	0.001	0.001	0.001	0.001	-1.21	0.23	7219	0.39
	Sn	0.002	0.002	0.001	0.001	-0.03	0.98	6862.5	0.88
	Ti	0.003	0.003	0.003	0.003	1.33	0.18	6398	0.45
	Zn	0.016	0.014	0.013	0.012	1.44	0.15	6165	0.23
	Zi	0.001	0.002	0.001	0.001	-0.16	0.87	6797	0.98
Dearborn	PM _{2.5}	8.618	9.123	7.950	7.350	-0.54	0.59	1827.5	0.76
	EC	0.572	0.497	0.502	0.432	1.41	0.16	1433	0.05*
	OC	2.035	2.045	2.065	1.864	-0.06	0.95	1725	0.70
	NH ₄ ⁺	0.564	0.606	0.380	0.300	-0.33	0.74	1665	0.39
	NO ₃ ⁻	1.509	1.580	0.800	0.575	-0.19	0.85	1635	0.31
	SO ₄ ²⁻	1.073	1.168	0.920	1.000	-0.81	0.42	1881.5	0.79
	S	0.382	0.400	0.328	0.317	-0.42	0.68	1819.5	0.96

	Al	0.028	0.024	0.023	0.018	0.53	0.60	1816	0.94
	Sb	0.004	0.001	0.005	0.001	2.01	0.05*	1431	0.04*
	Ba	0.006	0.005	0.002	0.001	0.40	0.69	1774	0.77
	BC	0.778	0.870	0.756	0.721	-1.08	0.28	1835	0.85
	Br	0.001	0.001	0.000	0.000	-0.23	0.82	1839	0.96
	Cd	0.001	0.001	0.000	-0.001	-0.08	0.93	1820	0.96
	Ca	0.155	0.091	0.100	0.068	2.54	0.01*	1295	<0.01*
	Ce	0.007	0.003	0.006	0.002	0.82	0.41	1696	0.49
	Cl ⁻	0.226	0.174	0.149	0.107	1.01	0.31	1633	0.31
	Cs	0.001	-0.001	0.000	0.002	0.78	0.43	1698	0.50
	Cr	0.002	0.005	0.001	0.002	-1.28	0.21	1792.5	0.97
	Co	0.000	0.000	0.000	0.000	0.88	0.38	1619	0.32
	Cu	0.026	0.014	0.020	0.009	4.00	<0.01*	974.5	<0.01*
	In	0.002	0.000	0.001	0.000	1.51	0.13	1530.5	0.12
	Fe	0.353	0.303	0.290	0.129	0.63	0.53	1273	<0.01*
	Pb	0.006	0.006	0.005	0.002	-0.04	0.97	1490.5	0.08
	Mg	0.034	0.023	0.019	0.016	1.35	0.18	1559.5	0.16
	Mn	0.010	0.005	0.007	0.004	3.25	<0.01*	1280.5	<0.01*
	Ni	0.001	0.003	0.001	0.001	-1.28	0.20	1999	0.28
	K ⁺	0.043	0.049	0.030	0.030	-0.73	0.47	1909.5	0.68
	Ru	0.001	0.000	0.000	0.000	2.03	0.04*	1548.5	0.14
	Se	0.001	0.001	0.001	0.001	1.84	0.07	1541	0.13
	Si	0.091	0.064	0.056	0.050	1.68	0.10	1609.5	0.25
	Ag	0.001	0.003	0.000	0.002	-1.52	0.13	2057.5	0.24
	Na ⁺	0.047	0.054	0.030	0.030	-0.67	0.51	1936	0.58
	Sr	0.001	0.001	0.000	0.000	0.88	0.38	1842	0.95
	Sn	0.004	-0.001	0.003	-0.004	2.39	0.02*	1417	0.03*
	Ti	0.005	0.002	0.003	0.002	2.83	0.01*	1335	<0.01*
	V	0.000	0.001	0.000	0.000	-1.41	0.16	2010.5	0.19
	Zn	0.068	0.036	0.032	0.014	2.03	0.04*	1195.5	<0.01*
	Zi	0.001	0.000	0.000	-0.001	0.56	0.57	1670	0.41
	PM _{2.5}	10.449	9.857	9.274	8.334	0.59	0.55	1462.5	0.23
	EC	0.692	0.533	0.573	0.478	2.69	<0.01*	1016.5	<0.01*
	OC	2.789	2.095	2.492	1.837	3.21	<0.01*	973	<0.01*
	NH ₄ ⁺	0.583	0.606	0.415	0.305	-0.17	0.86	1491.5	0.29
	NO ₃ ⁻	1.653	1.503	1.065	0.570	0.40	0.69	1129.5	<0.01*
	SO ₄ ²⁻	1.194	1.192	0.885	1.000	0.02	0.99	1695	0.95
	S	0.408	0.429	0.299	0.352	-0.43	0.67	1759	0.67
South-West High School	Al	0.077	0.041	0.033	0.031	1.59	0.12	1706	0.90
	Sb	0.002	0.005	0.000	0.004	-1.69	0.09	1985	0.09
	Ba	0.006	0.006	0.004	0.007	0.13	0.90	1704	0.91
	BC	0.771	0.887	0.726	0.723	-1.31	0.19	1746	0.60
	Br	0.001	0.001	0.000	0.000	0.06	0.96	1762.5	0.60
	Cd	0.002	0.002	0.000	0.000	0.03	0.97	1700	0.92
	Ca	0.102	0.213	0.072	0.093	-2.30	0.02*	1872	0.30
	Ce	-0.002	-0.003	-0.004	0.000	0.32	0.75	1667	0.94
	Cl ⁻	0.237	0.178	0.128	0.075	1.21	0.23	1317	0.04*
	Cs	0.001	0.003	0.000	0.001	-0.63	0.53	1775	0.61
	Cr	0.001	0.002	0.001	0.001	-0.96	0.34	1694	0.95

Cu	0.008	0.013	0.008	0.013	-3.18	<0.01*	2310	<0.01*
In	0.001	0.002	0.000	0.002	-0.36	0.72	1794.5	0.54
Fe	0.180	0.126	0.140	0.084	2.25	0.03*	1141	<0.01*
Pb	0.004	0.004	0.005	0.003	0.20	0.84	1568.5	0.53
Mg	0.020	0.023	0.000	0.009	-0.45	0.65	1758.5	0.67
Mn	0.005	0.004	0.004	0.003	1.33	0.18	1300	0.03*
Ni	0.001	0.001	0.000	0.000	-0.27	0.79	1705.5	0.89
K ⁺	0.124	0.040	0.040	0.030	1.77	0.08	1314.5	0.04*
Ru	0.000	0.000	0.000	0.000	0.18	0.86	1653.5	0.88
Se	0.001	0.001	0.001	0.001	0.60	0.55	1605	0.67
Si	0.080	0.135	0.059	0.071	-2.09	0.04*	1972.5	0.11
Ag	0.001	0.001	0.000	0.000	-0.14	0.89	1693.5	0.95
Na ⁺	0.033	0.036	0.030	0.020	-0.39	0.70	1646	0.84
Sr	0.001	0.002	0.000	0.001	-2.32	0.02*	2012	0.07
Sn	0.001	0.001	0.001	0.001	-0.25	0.80	1730	0.79
Ti	0.016	0.004	0.004	0.002	1.95	0.06	1372.5	0.09
V	0.001	0.000	0.000	0.000	0.71	0.48	1804.5	0.41
Zn	0.029	0.020	0.023	0.015	2.40	0.02*	1268	0.02*
Zi	0.001	0.001	0.000	0.000	-0.02	0.98	1707	0.89

Figure S2. Trends of monthly median levels of selected species for 1-year pre-pandemic and pandemic periods at Allen Park.

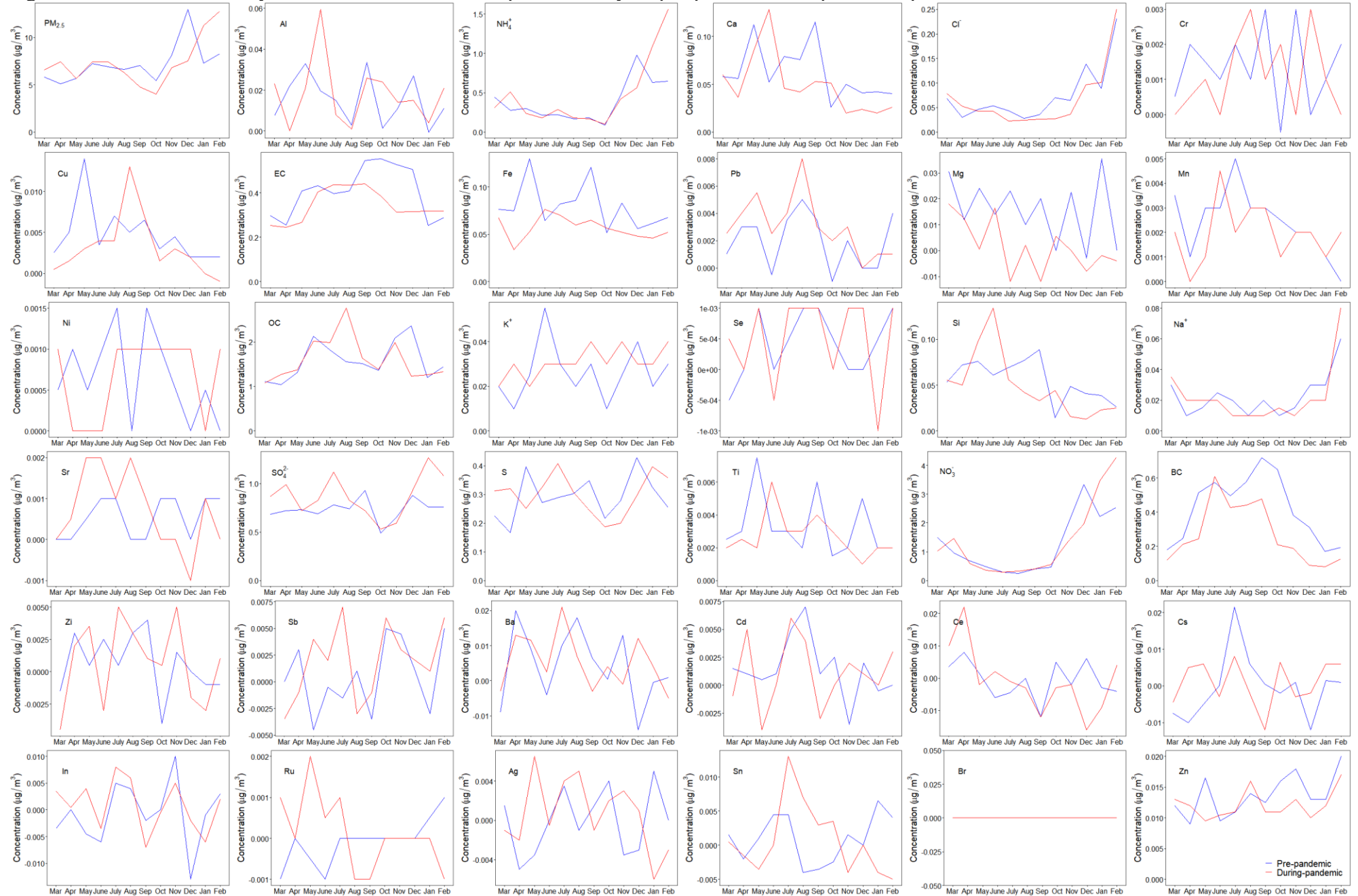


Figure S3. Trends of monthly median concentrations selected species for 1-year pre-pandemic and pandemic periods at Dearborn.

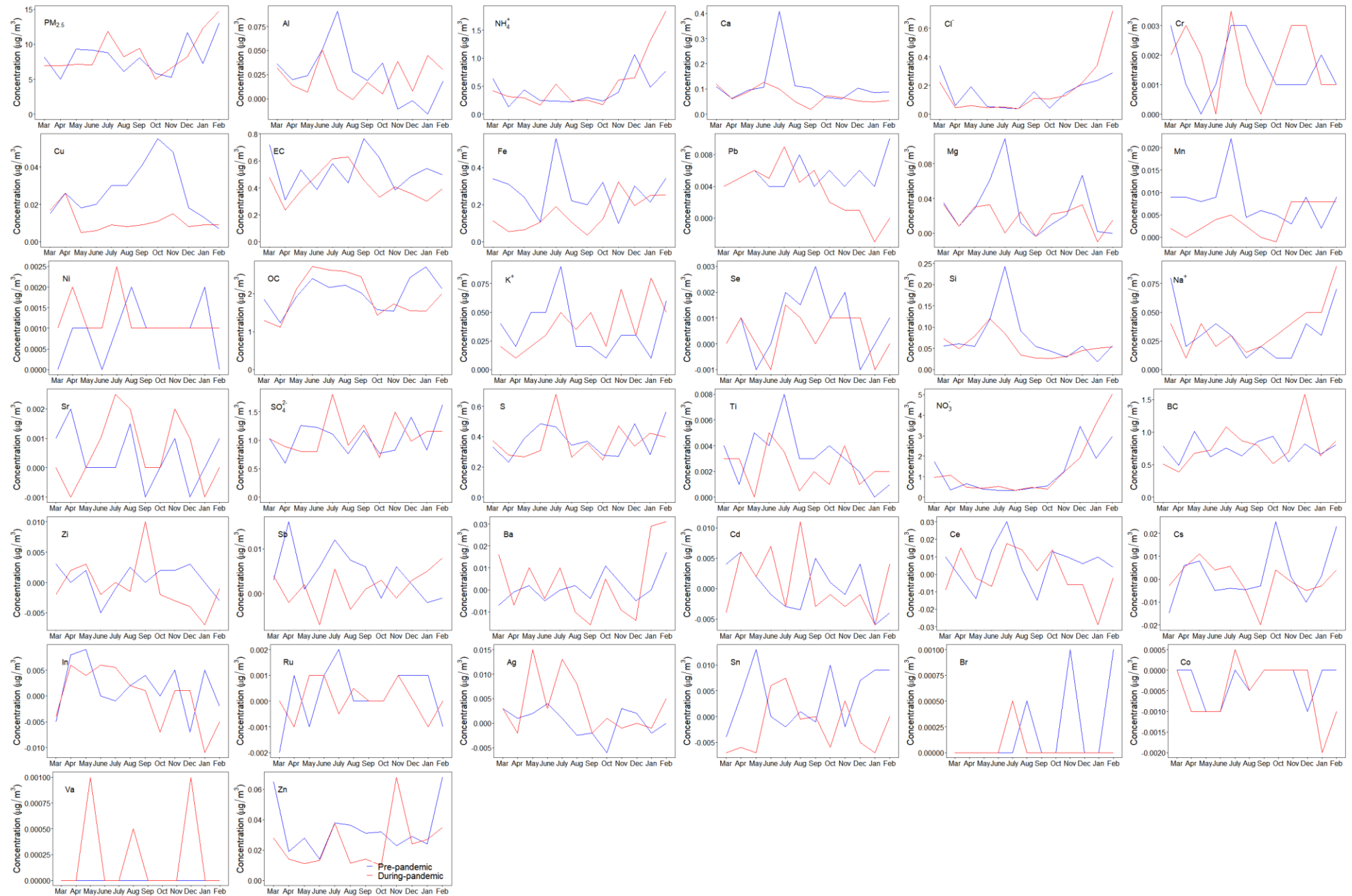


Figure S4. Trends of monthly median concentrations for selected species for 1-year pre-pandemic and pandemic periods at SWHS.

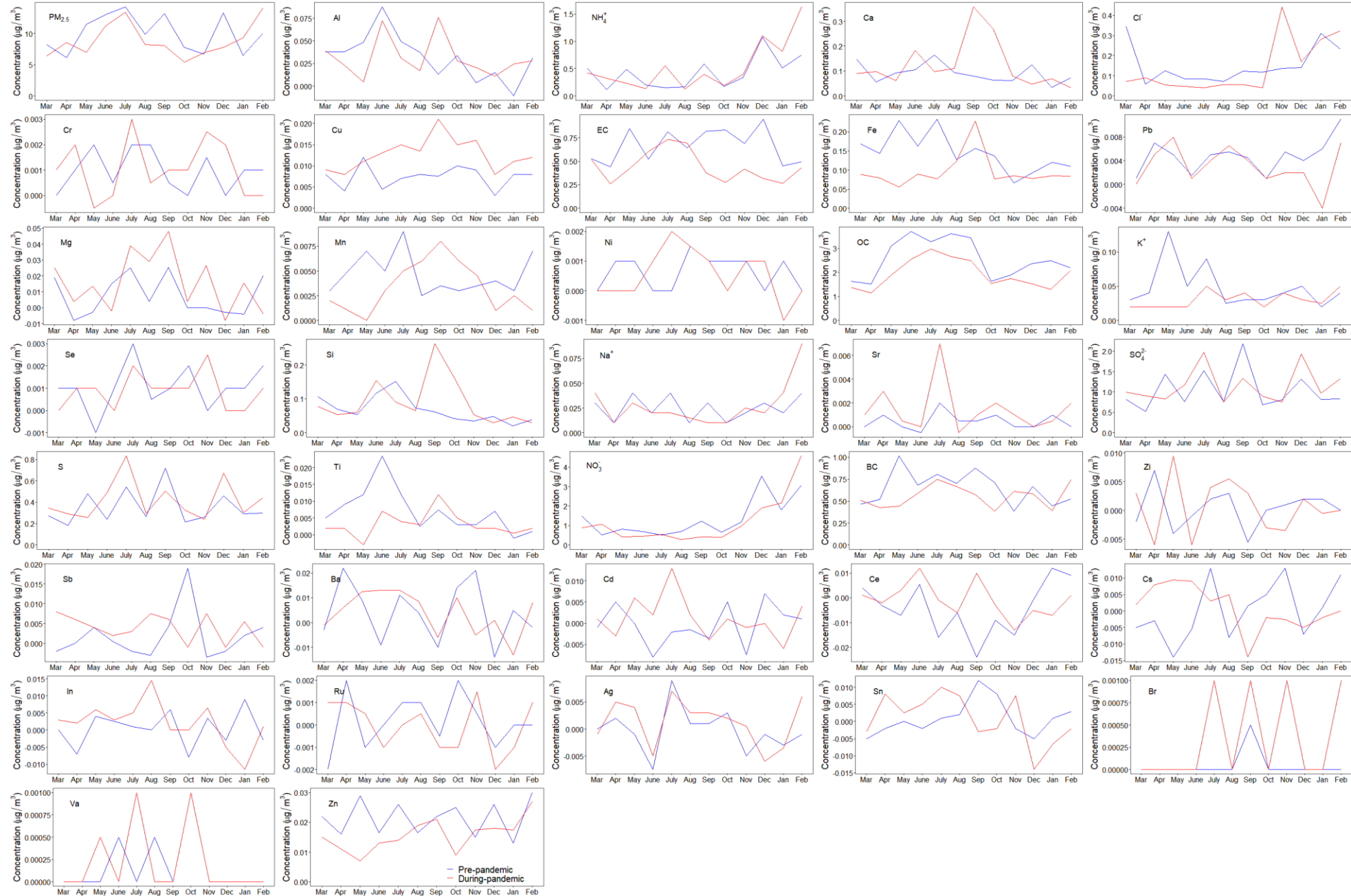
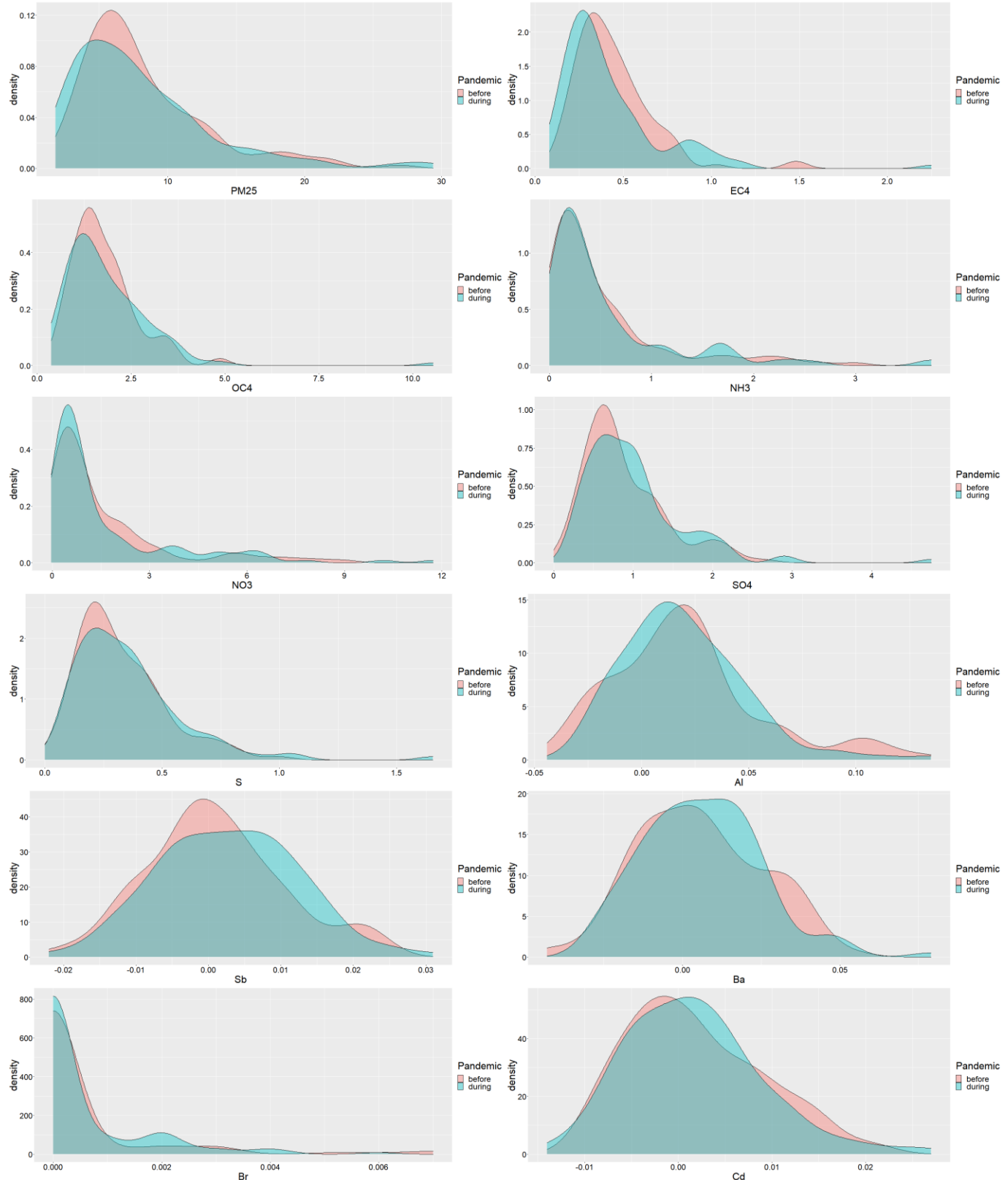
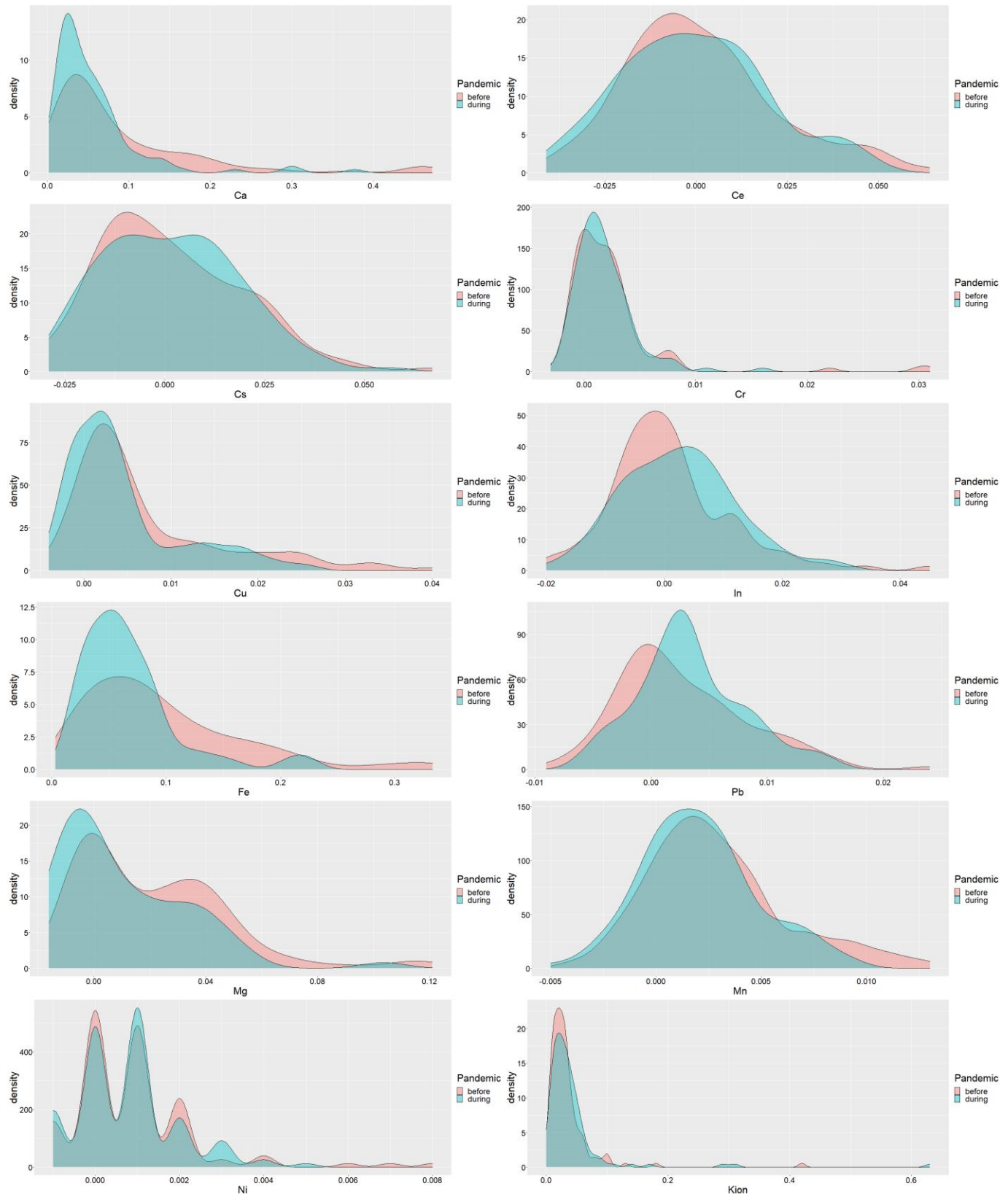


Figure S5. Density plots comparing before and during the pandemic periods for selected species at Allen Park. Continued across 3 pages.





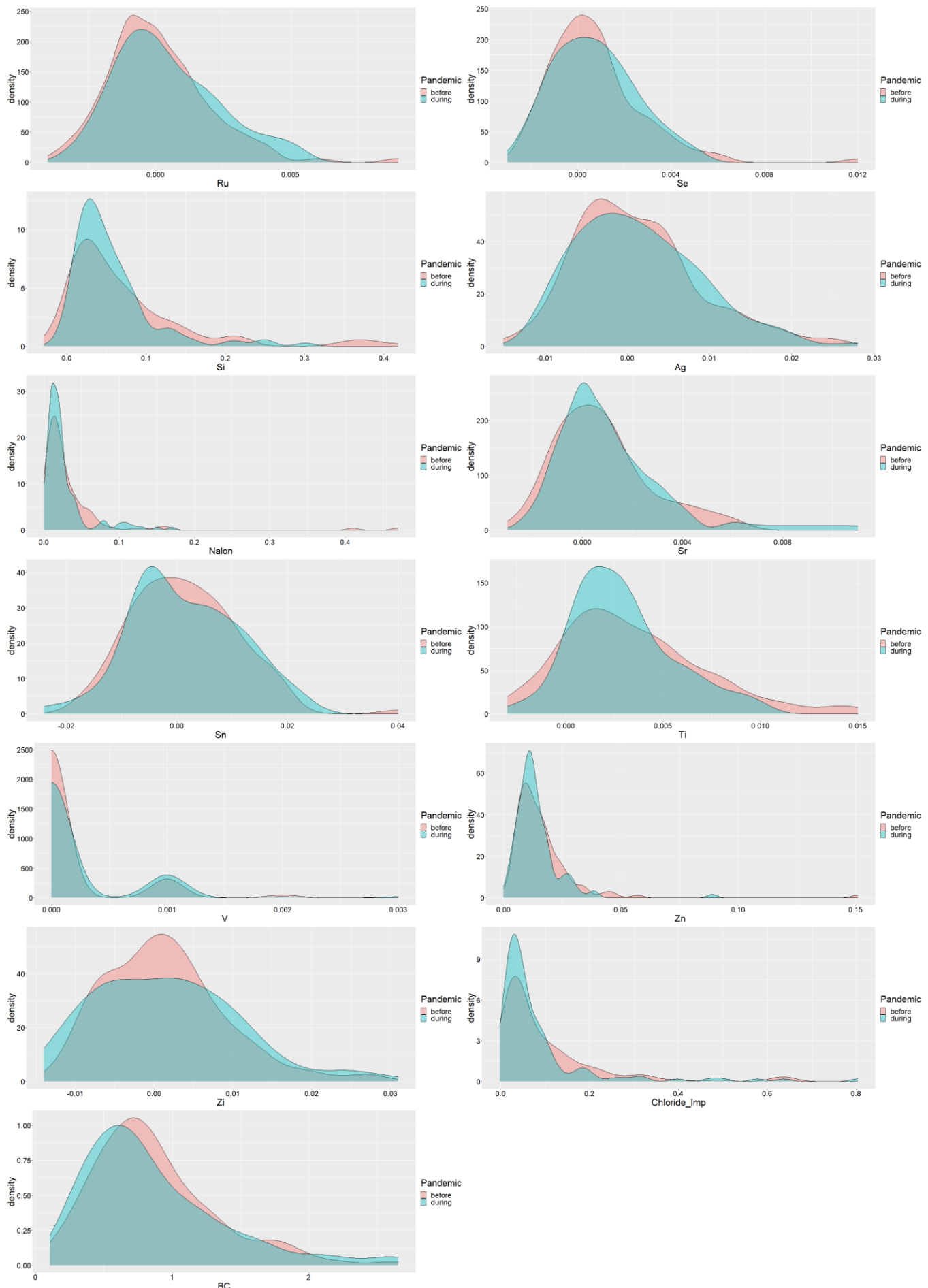
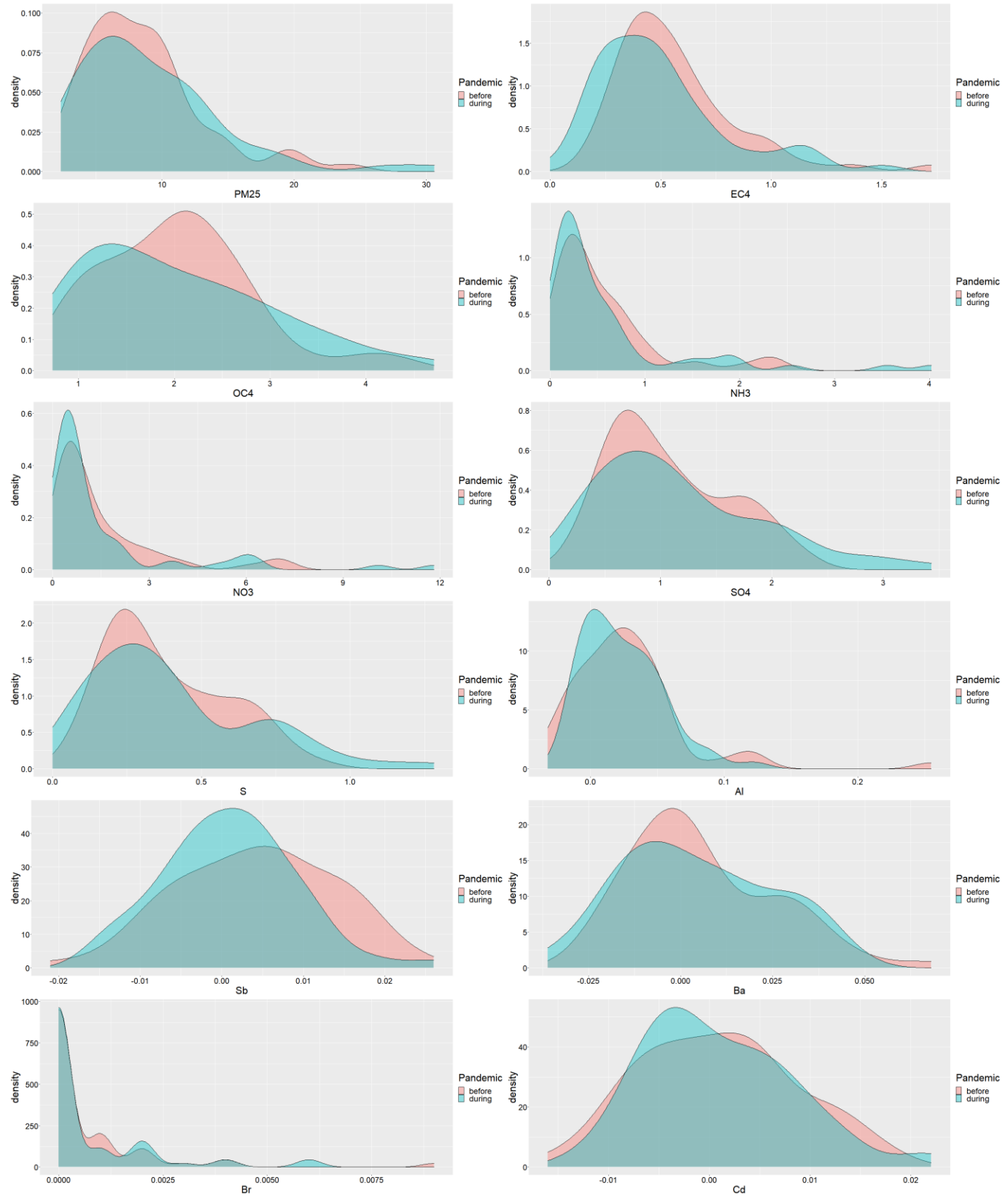
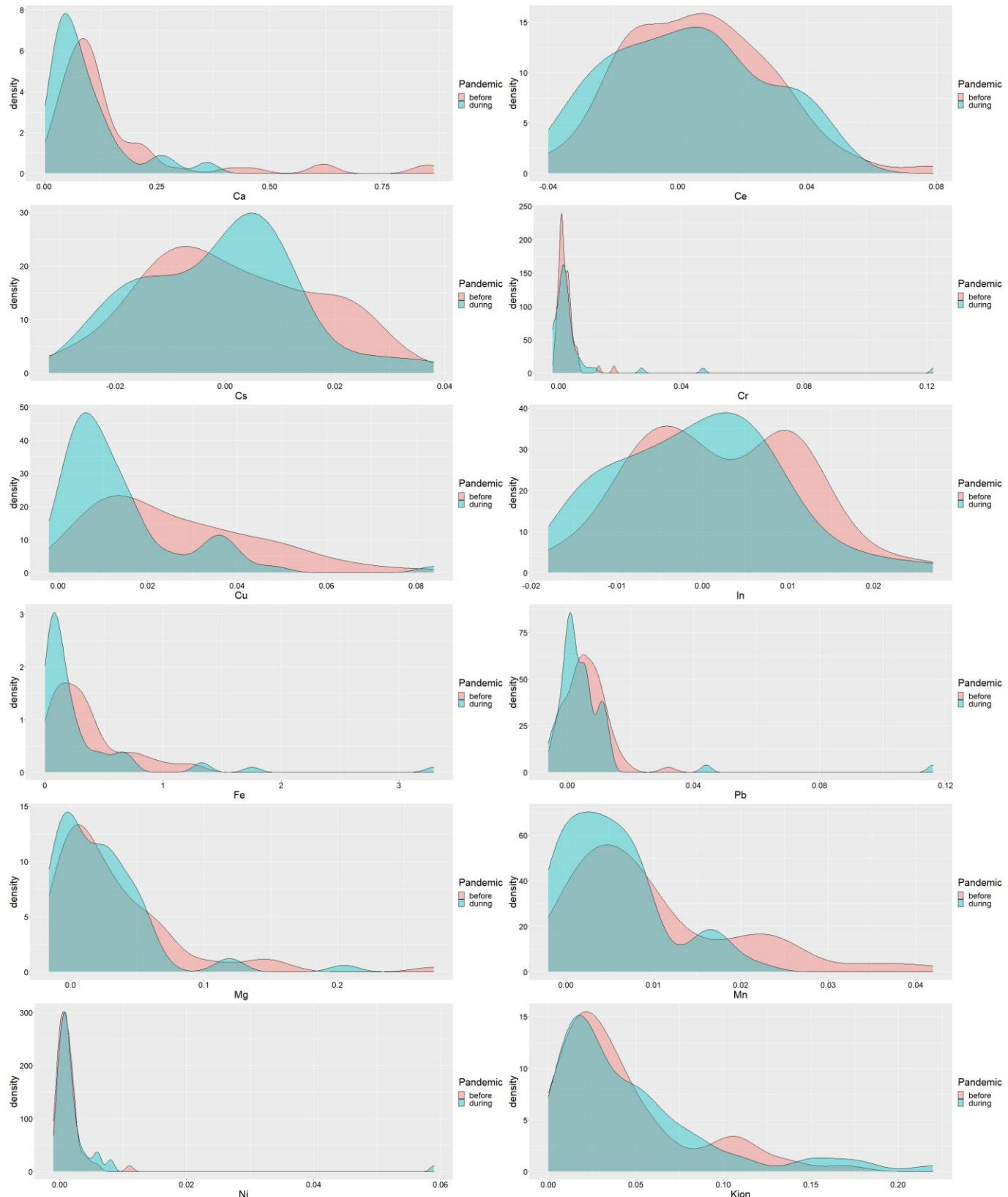


Figure S6. Density plots comparing before and during the pandemic periods for selected species at Dearborn. Continued across 3 pages.





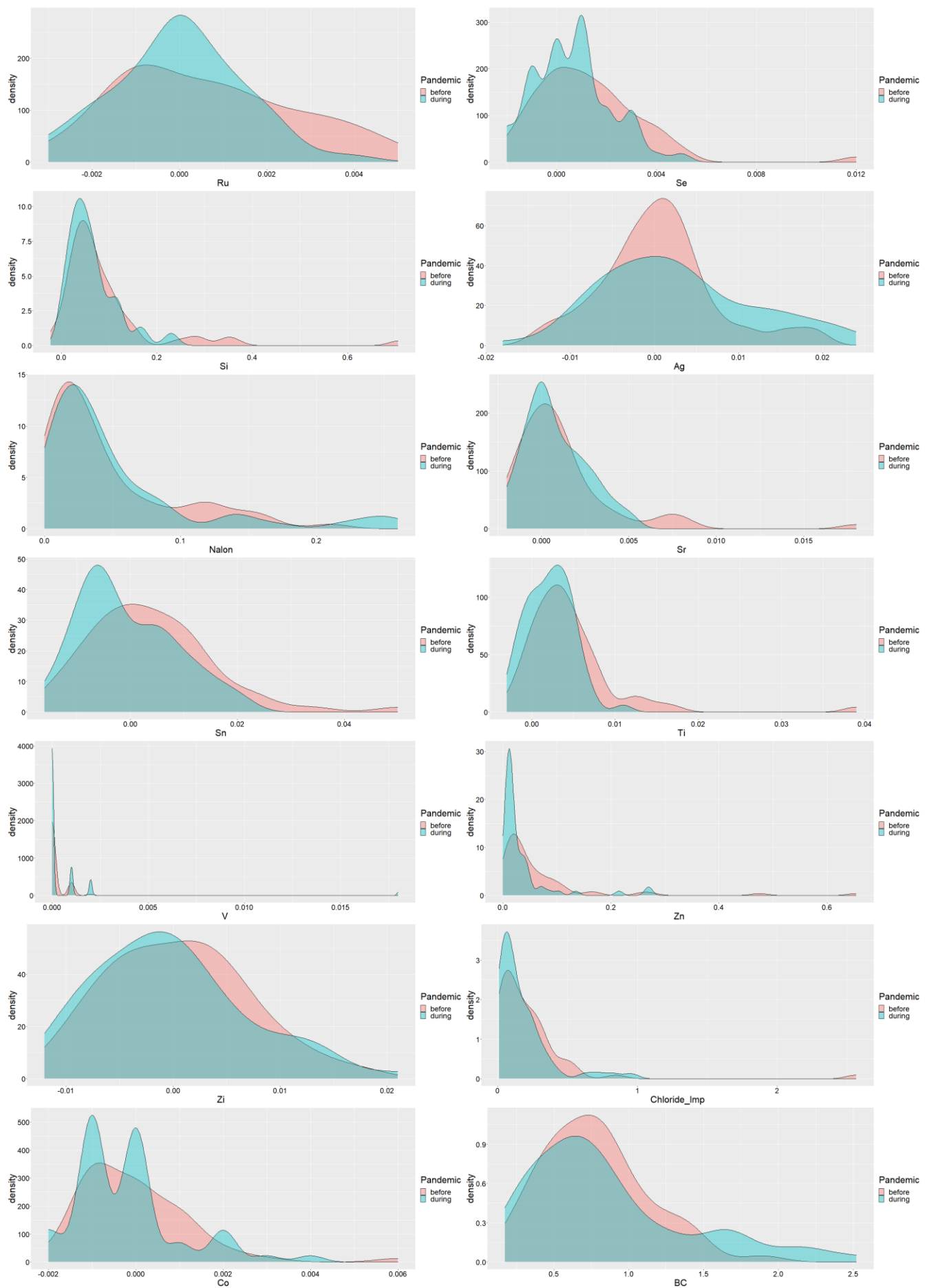
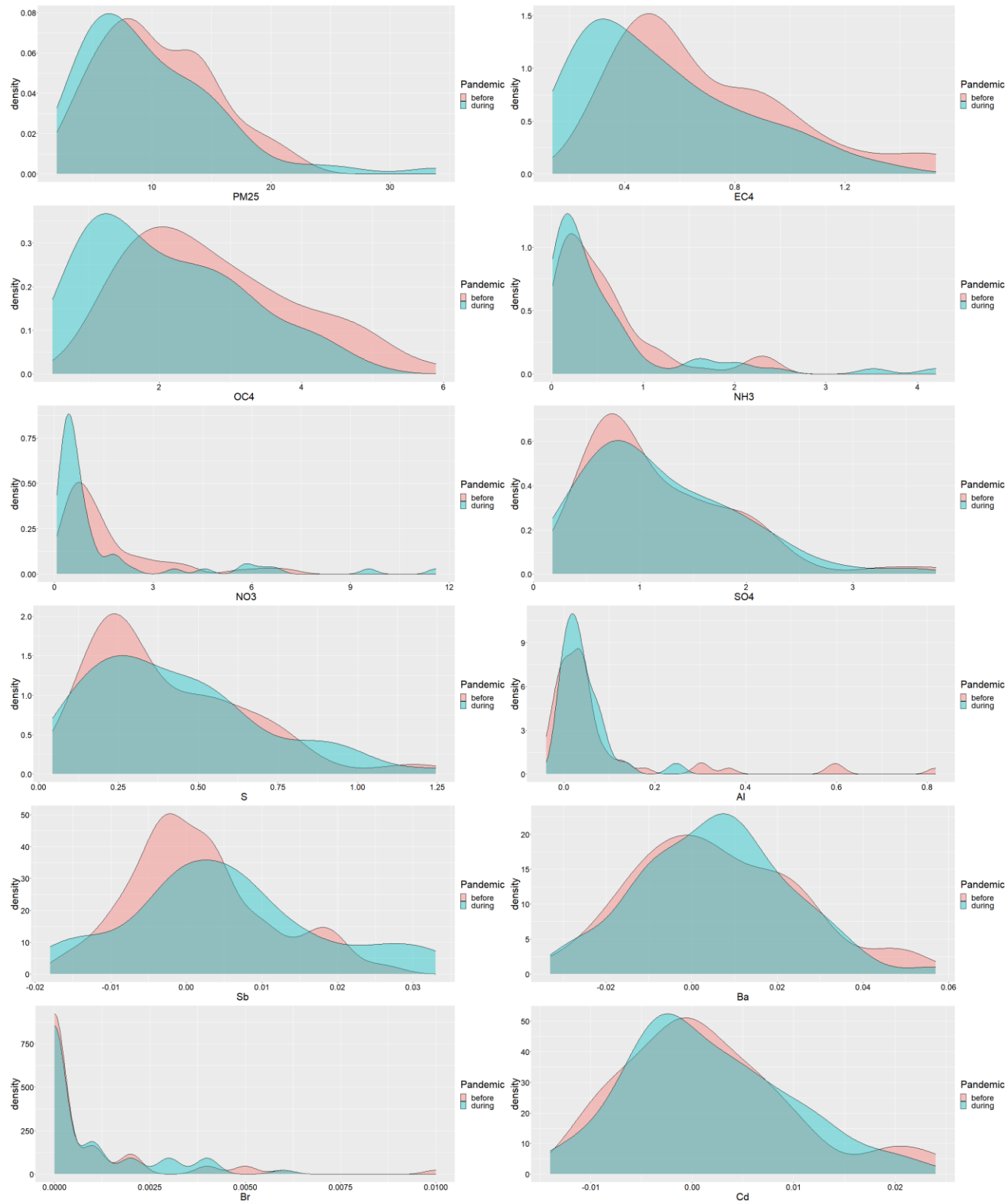
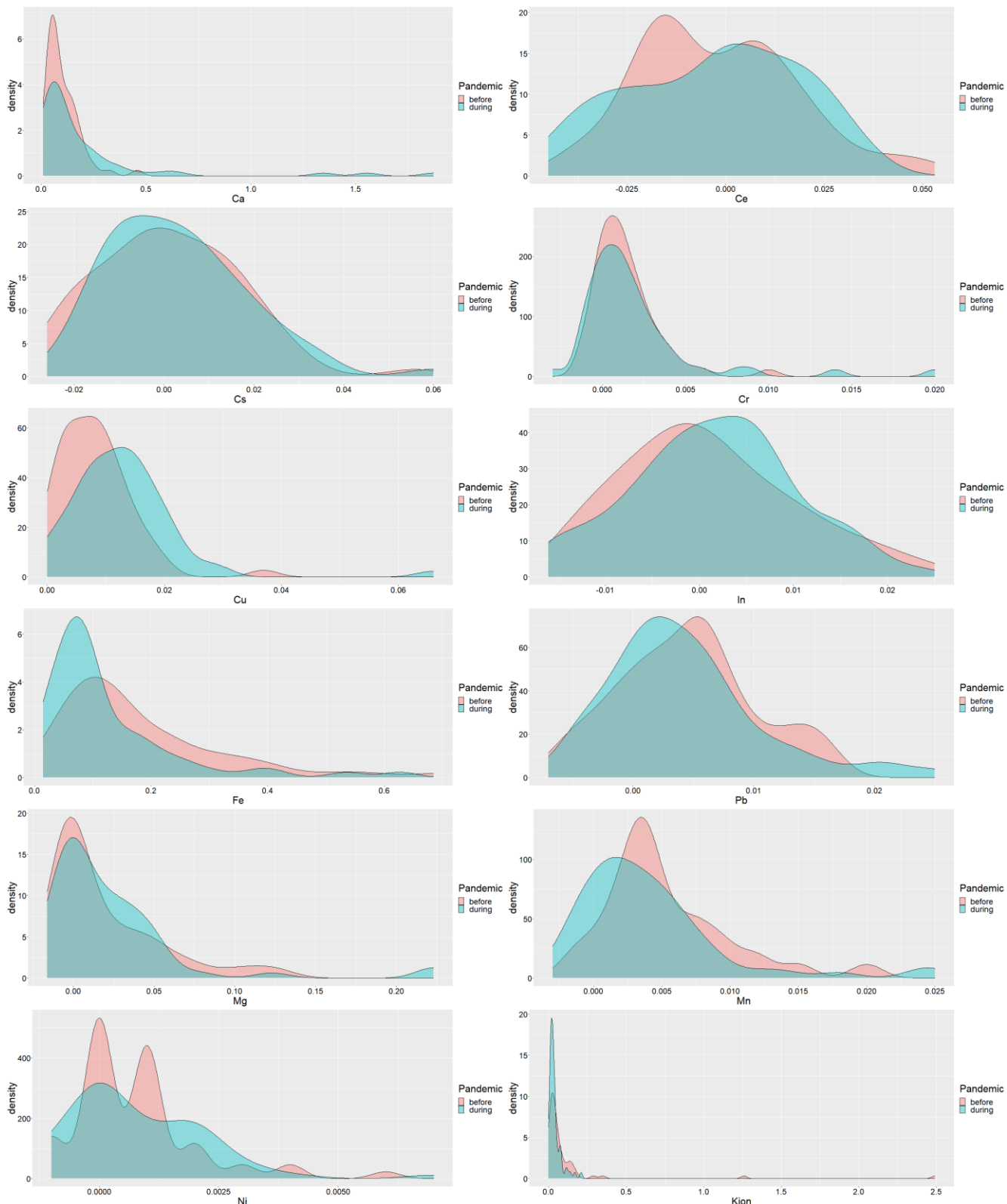


Figure S7. Density plots comparing before and during the pandemic periods for selected species at SWHS.
Continued across 3 pages.





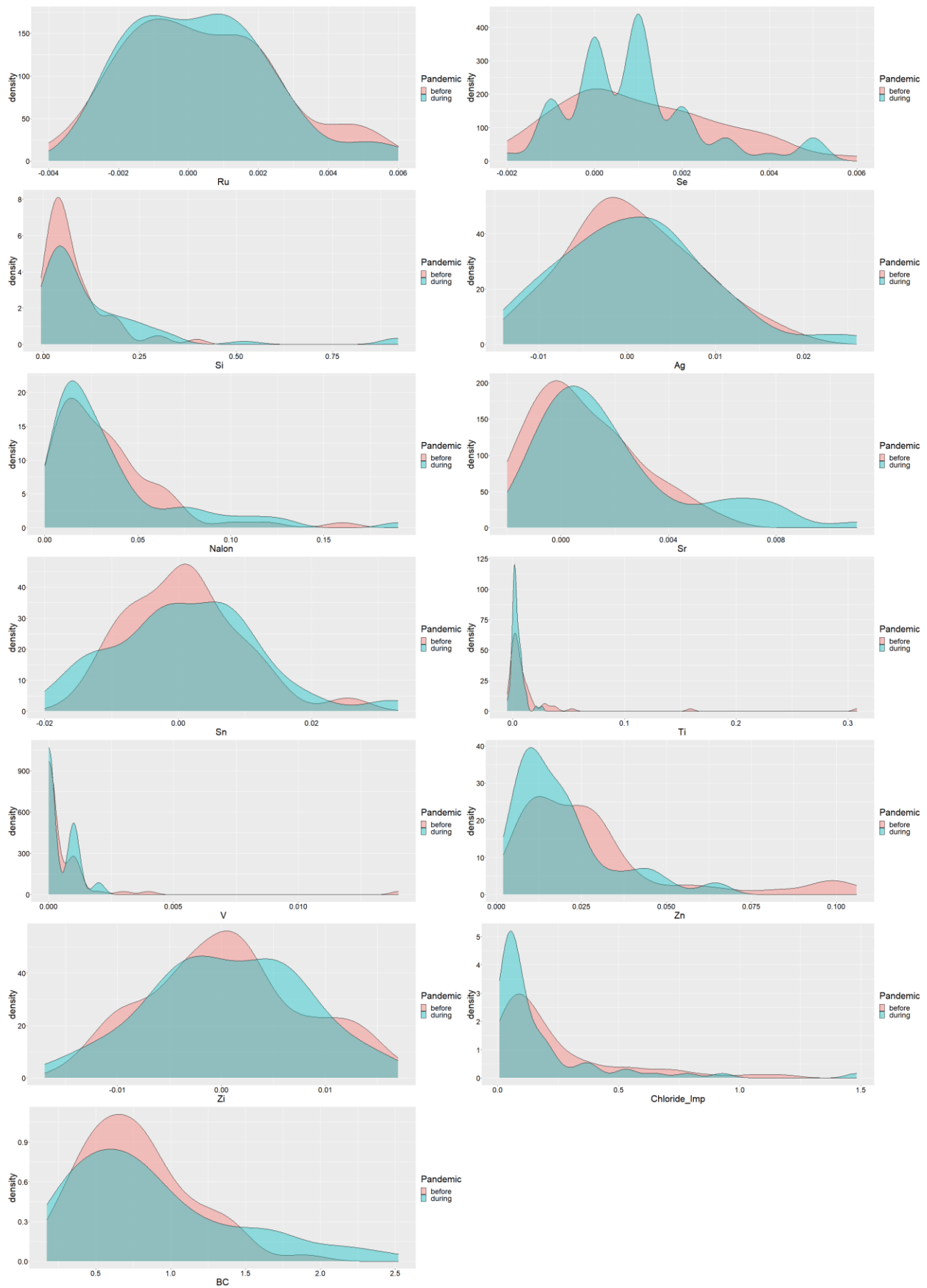


Figure S8. Factor profiles for approach 1 for pre-pandemic and lockdown periods at Allen Park.

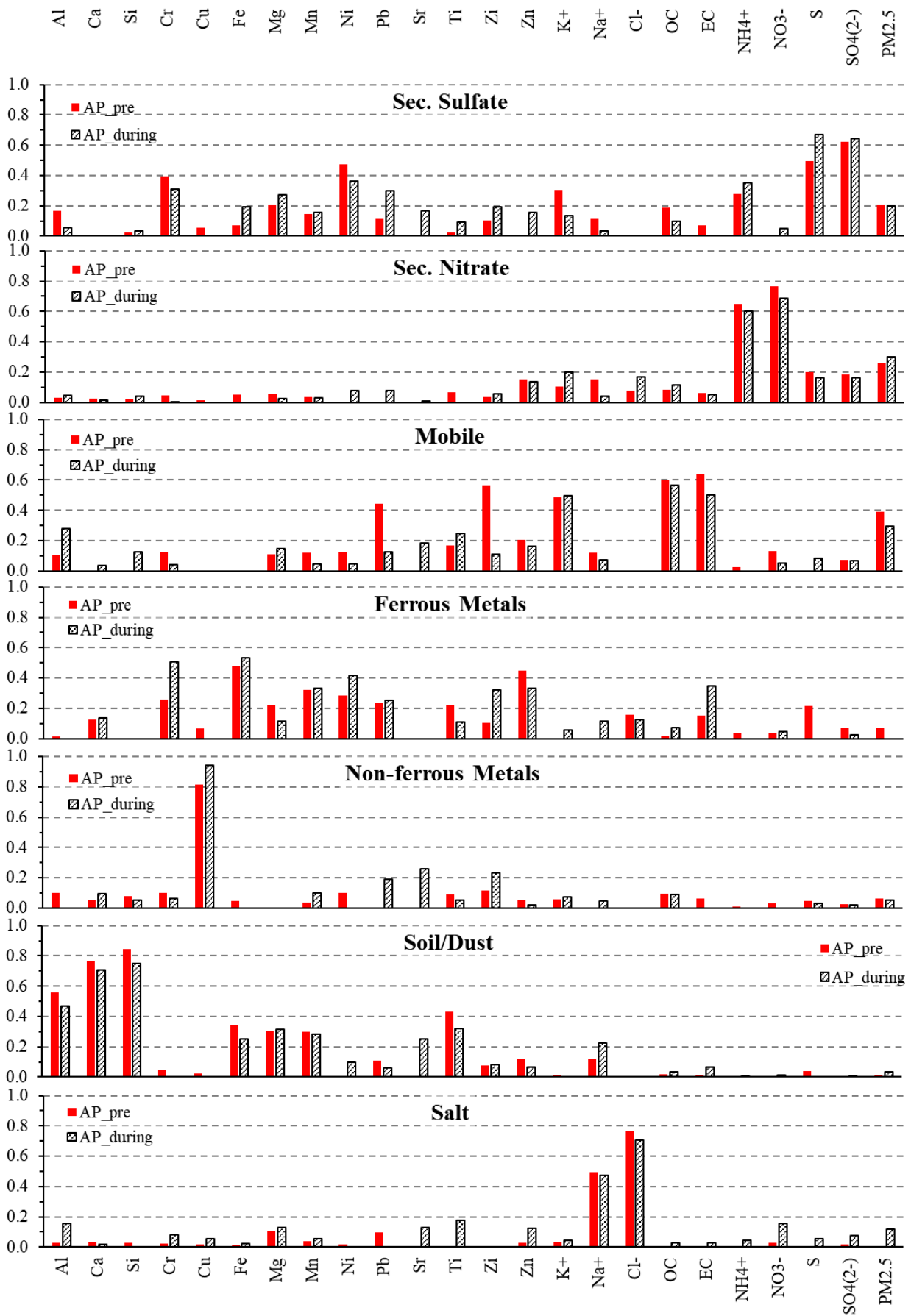


Figure S9. Factor profiles for approach 1 for pre-pandemic and pandemic periods at Dearborn.

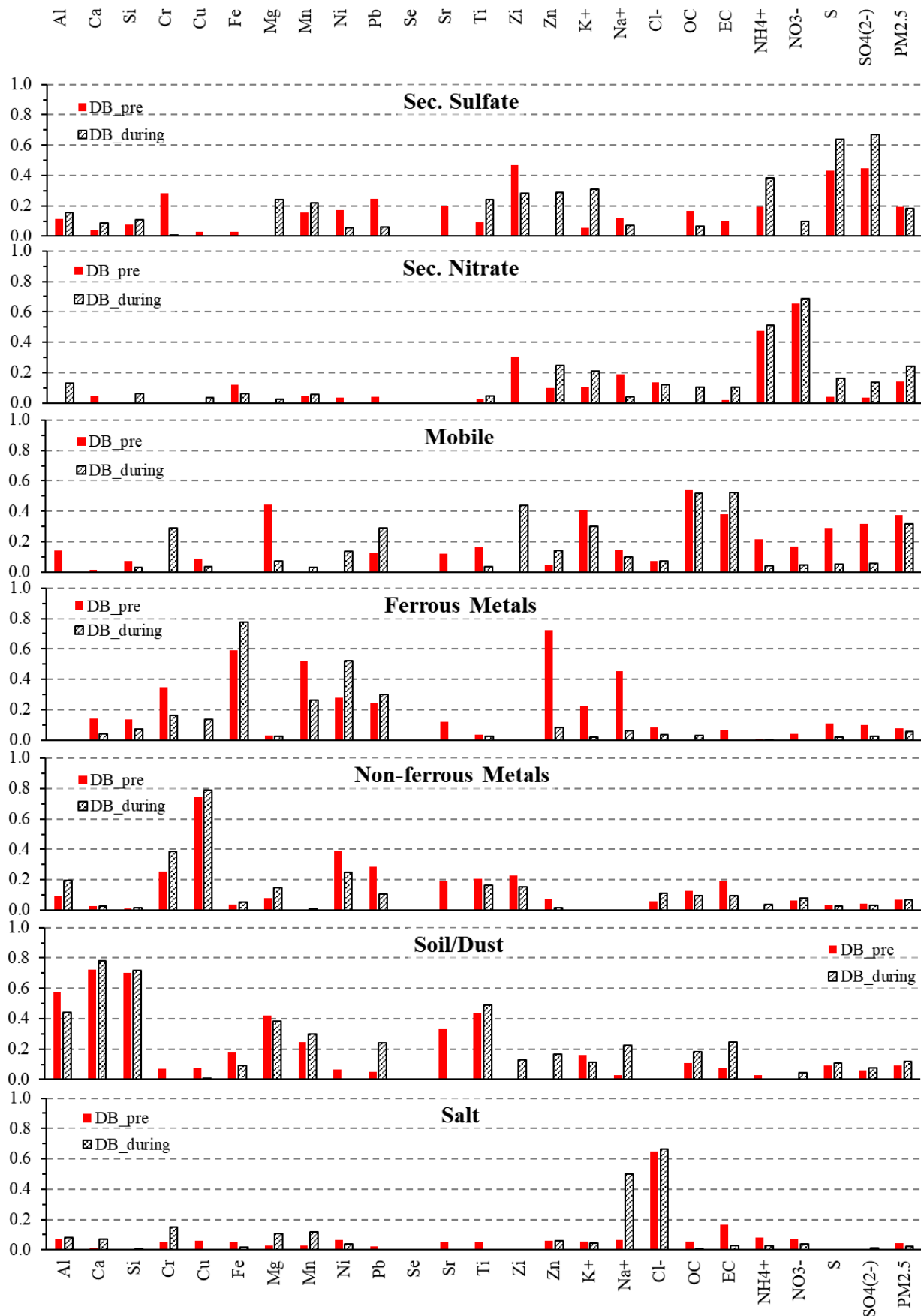


Figure S10. Factor profiles for approach 1 for pre-pandemic and pandemic periods at SWHS site.

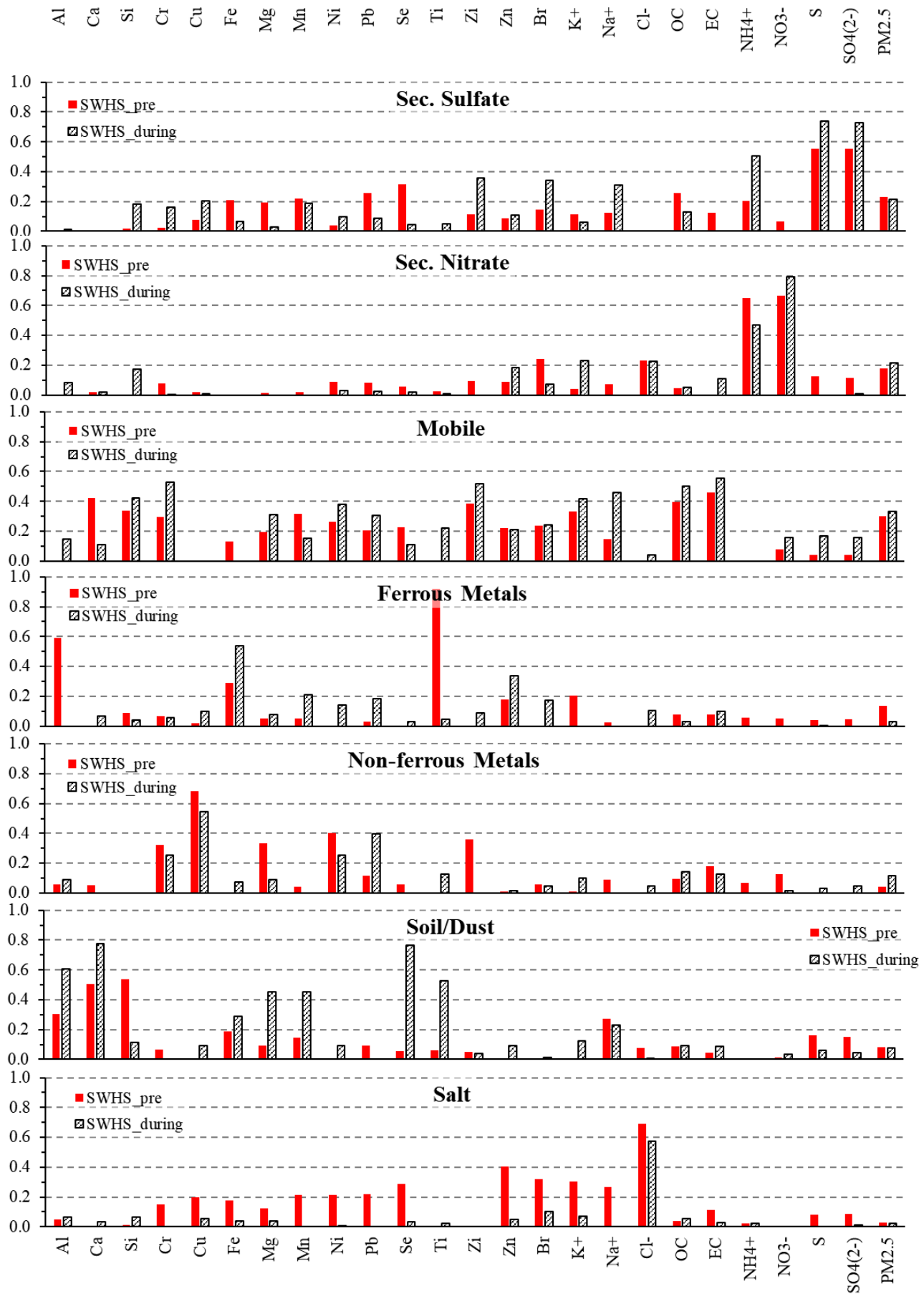


Figure S11. Factor profiles of approach 2A and 3 for pre-pandemic and pandemic periods. Four sets of profiles are shown: Colored bars are for three individual sites using approach 3; hatched bar is profile for combined dataset using approach 2A.

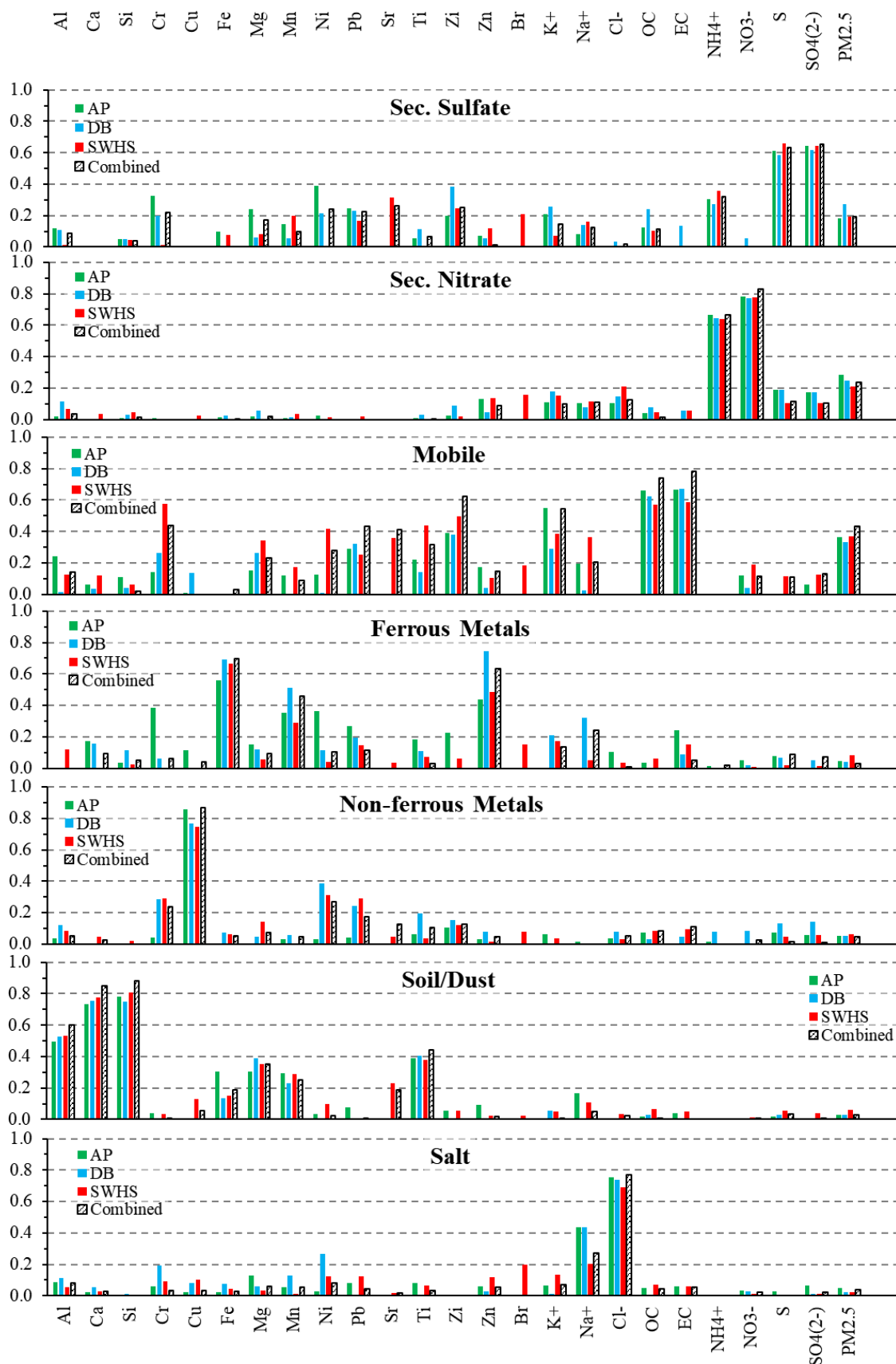


Figure S12. Annual wind rose for Detroit City Airport (Jan. 1, 2017 to Dec. 31, 2021).
Generated using Midwestern Regional Climate Center cli-MATE: MRCC Application Tools Environment
(<https://mrcc.purdue.edu/CLIMATE/Hourly/WindRose2.jsp>)

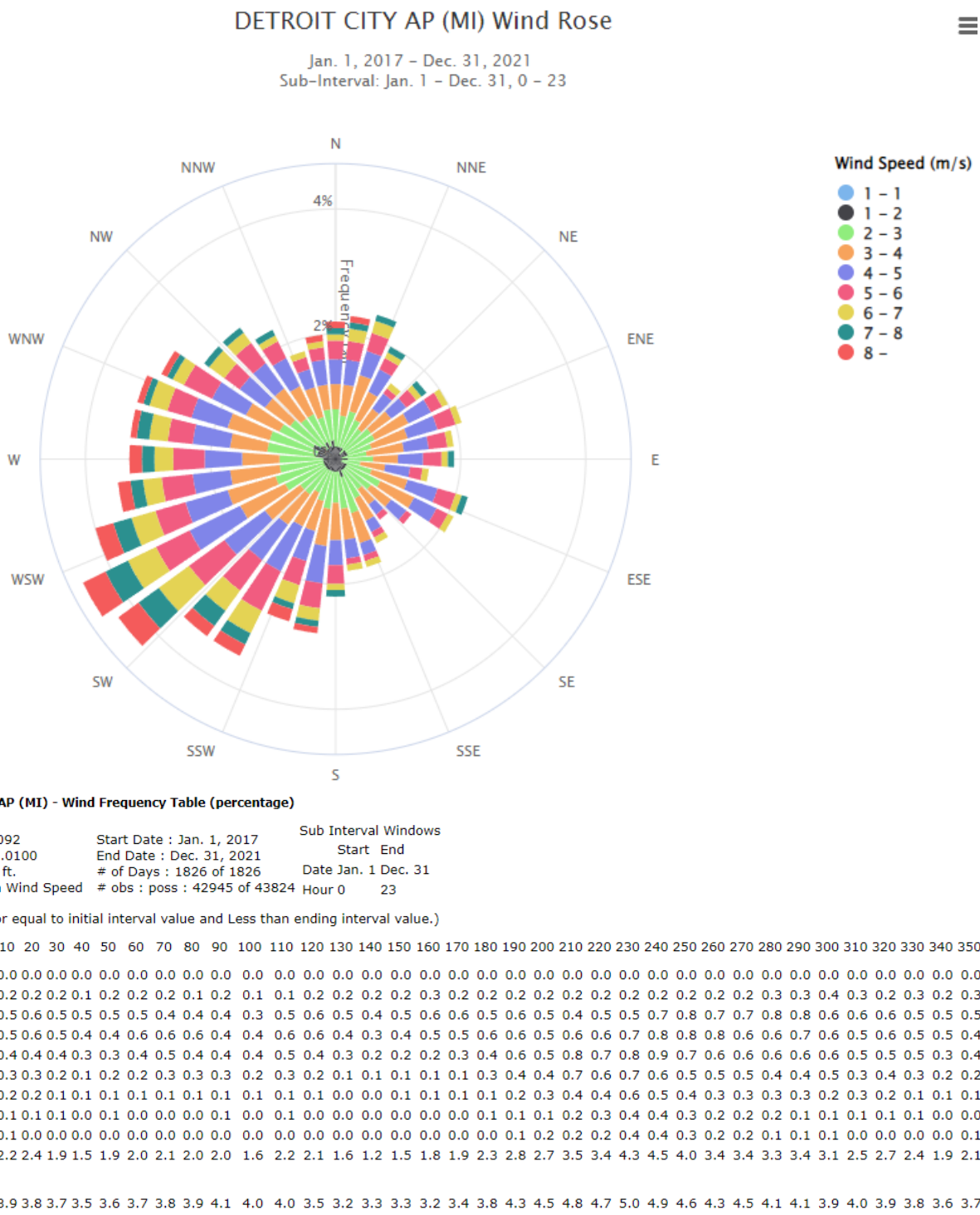


Figure S13. Seasonal wind roses for Detroit City Airport.

Average wind speed in winter, spring, summer, and fall is 4.1, 4.0, 3.1, and 3.5 m/s, respectively; calms (wind speed less than 1 m/s) represent 6.6, 8.0, 13.5 and 11.6% of the time, respectively.

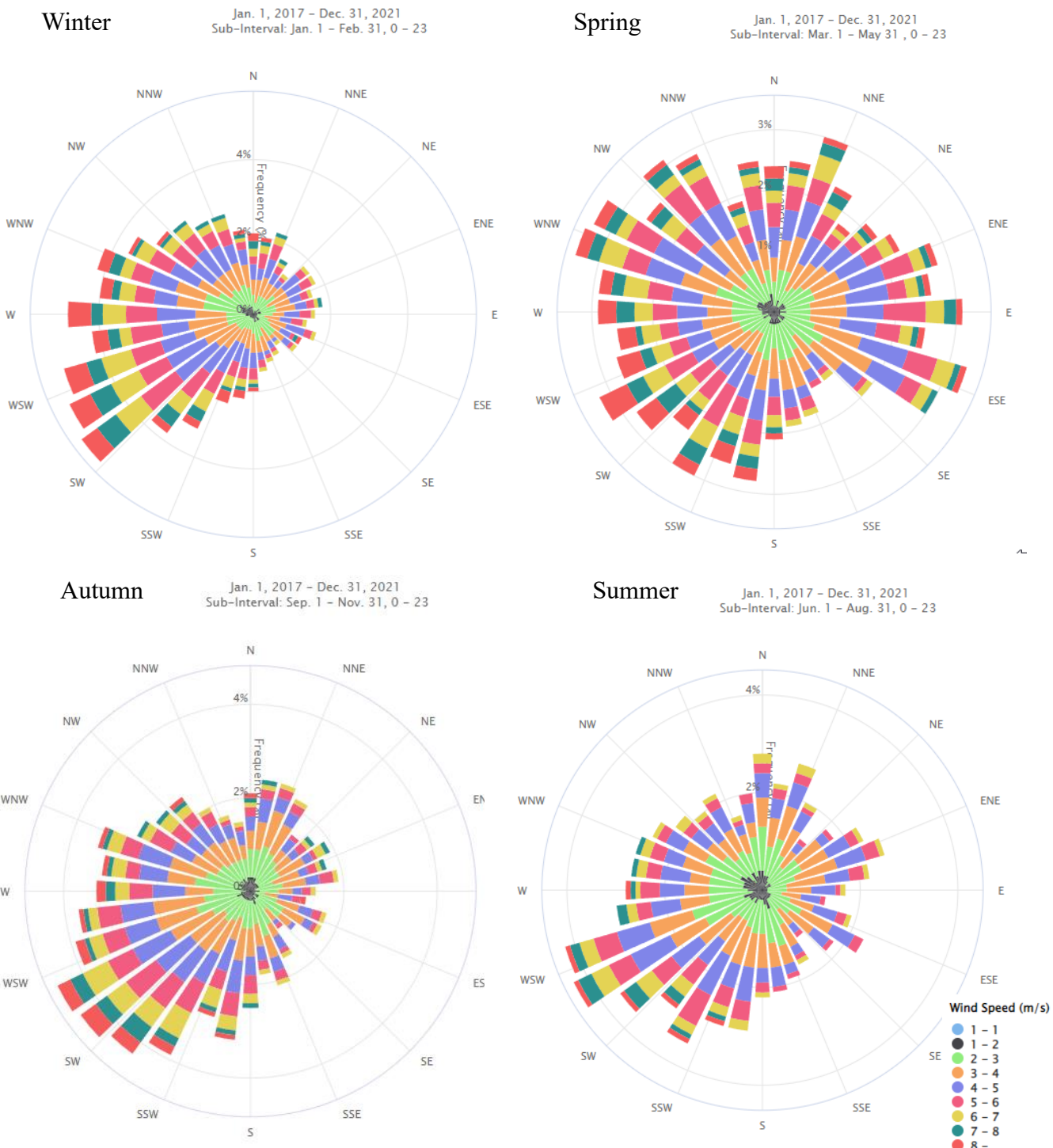
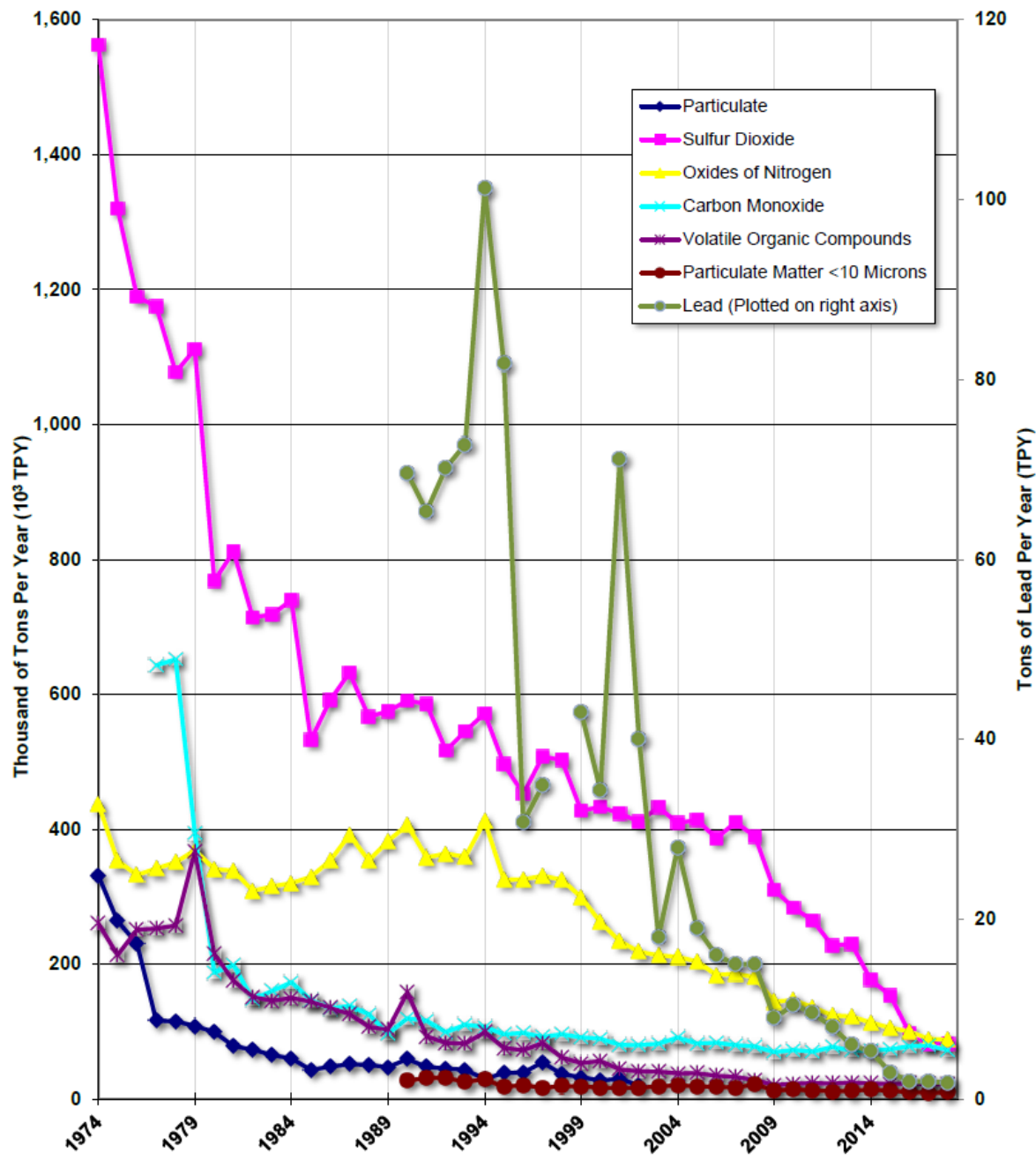


Figure S14. Michigan state-wide stationary (point) source emission trends from 1974 to 2018.
From Michigan Department of Environment, Energy and Great Lakes, 2019.



Report notes: 1) Estimating methodologies, emission factors, and data availability can vary year to year. Caution should be exercised when evaluating trends in emission estimations and should only be interpreted in a qualitative manner; 2) The criteria emissions estimate data presented here represents the data reported from the facilities and is subject to limited quality assurance efforts by EGLE to identify, verify, and correct outlier data.

Source: Michigan Air Emissions Reporting System (MAERS), Michigan Dept. of Environment, Great Lakes, and Energy - Air Quality Division Revised December 16, 2019 <https://www.michigan.gov/egle-/media/Project/Websites/egle/Documents/Programs/AQD/monitoring/emission-trends-stationary-point-sources.pdf?rev=b9e63faa8d254877af2e2892d3d31935&hash=E1DD451569759D417876D7CB4BC339F8>

Reference

1. Viana, M.; Pandolfi, M.; Mingüillón, M.C.; Querol, X.; Alastuey, A.; Monfort, E.; Celades, I.; Inter-comparison of receptor models for PM source apportionment: Case study in an industrial area. *Atmos. Environ.* **2008**, *42*, 3820–3832. <https://doi.org/10.1016/j.atmosenv.2007.12.056>.
2. Henry, R.C.; Kim, B.M. The USEPA/DRI Chemical Mass Balance Receptor Model, CMB 7.0 J.G. Watson, N.F. Robinson, and J.C. Chow. *Environ. Softw.* **1990**, *5*, 12. <https://doi.org/10.1016/0266-983890015-X>.
3. Chow, J.C.; Watson, J.G. Review of PM 2.5 and PM 10 Apportionment for Fossil Fuel Combustion and Other Sources by the Chemical Mass Balance Receptor Model. *Energy Fuels* **2002**, *16*, 222–260. <https://doi.org/10.1021/ef0101715>.
4. Keats, A.; Cheng, M.-T.; Yee, E.; Lien, F.-S. Bayesian treatment of a chemical mass balance receptor model with multiplicative error structure. *Atmos. Environ.* **2009**, *43*, 510–519. <https://doi.org/10.1016/j.atmosenv.2008.10.031>.
5. Comero, S.; Capitani, L.; Gawlik, B.M. Positive Matrix Factorisation (PMF). In *An Introduction to the Chemometric Evaluation of Environmental Monitoring Data Using PMF*; European Commission Joint Research Centre, Office for Official Publications of the European Communities: Luxembourg, 2009; p. 58.
6. Norris, G.; Duvall, R.; Brown, S.; Bai, S. *Positive Matrix Factorization (PMF) 5.0 Fundamentals and User Guide*; US Environmental Protection Agency: Washington, DC, USA, 2014; p. 136.
7. Kim, I.S.; Wee, D.; Kim, Y.P.; Lee, J.Y. Development and application of three-dimensional potential source contribution function (3D-PSCF). *Environ. Sci. Pollut. Res.* **2016**, *23*, 16946–16954. <https://doi.org/10.1007/s11356-016-6787-x>.
8. Hsu, Y.K.; Holsen, T.M.; Hopke, P.K.; Comparison of hybrid receptor models to locate PCB sources in Chicago. *Atmos. Environ.* **2003**, *37*, 545–562. <https://doi.org/10.1016/S1352-231000886-5>.
9. Reff, A.; Eberly, S.I.; Bhave, P.V. Receptor Modeling of Ambient Particulate Matter Data Using Positive Matrix Factorization: Review of Existing Methods. *J. Air Waste Manag. Assoc.* **2007**, *57*, 146–154. <https://doi.org/10.1080/10473289.2007.10465319>.
10. Buzcu-Guven, B.; Brown, S.G.; Frankel, A.; Hafner, H.R.; Roberts, P.T. Analysis and Apportionment of Organic Carbon and Fine Particulate Matter Sources at Multiple Sites in the Midwestern United States. *J. Air Waste Manag. Assoc.* **2007**, *57*, 606–619. <https://doi.org/10.3155/1047-3289.57.5.606>.
11. Gildemeister, A.E.; Hopke, P.K.; Kim, E. Sources of fine urban particulate matter in Detroit, MI. *Chemosphere* **2007**, *69*, 1064–1074. <https://doi.org/10.1016/j.chemosphere.2007.04.027>.
12. Brown, S.G.; Eberly, S.; Paatero, P.; Norris, G.A. Methods for estimating uncertainty in PMF solutions: Examples with ambient air and water quality data and guidance on reporting PMF results. *Sci. Total Environ.* **2015**, *518–519*, 626–635. <https://doi.org/10.1016/j.scitotenv.2015.01.022>.
13. Li, Z.; Hopke, P.K.; Husain, L.; Qureshi, S.; Dutkiewicz, V.A.; Schwab, J.J.; Drewnick, F.; Demerjian, K.L. Sources of fine particle composition in New York city. *Atmos. Environ.* **2004**, *38*, 6521–6529. <https://doi.org/10.1016/j.atmosenv.2004.08.040>.
14. Kim, E.; Hopke, P.K. Identification of Fine Particle Sources in Mid-Atlantic US Area. *Water Air Soil Pollut.* **2005**, *168*, 391–421. <https://doi.org/10.1007/s11270-005-1894-1>.
15. Sampling Methods for All Parameters|Air Quality System|US EPA. 2022. Retrieved 28 August 2022. Available online: https://aqs.epa.gov/aqsweb/documents/codetables/methods_all.html.